FIBREGY

This project has received funding from the European Union's Horizon 2020 research and innovation programme under grant agreement No 952966.

Development, engineering, production and life cycle management of improved FIBRE-based material solutions for the structure and functional components of large offshore wind enerGY and tidal power platforms

D6.3 (WP6): Construction of the turbine housing demonstrator

Responsible Partner: INEGI

Contributor(s): INEGI, TSI, TIDETEC

This project has received funding from the European Union's Horizon 2020 research and innovation programme under grant agreement No 952966.

DOCUMENT INFORMATION TABLE

CONTRACT NUMBER:	952966
PROJECT ACRONYM:	FIBREGY
PROJECT COORDINATOR:	Borja Serván Camas
DOCUMENT RESPONSIBLE	INEGI
DELIVERABLE TYPE:	Report
DOCUMENT TITLE:	Construction of the turbine housing demonstrator
DOCUMENT ID:	D6.3
DISSEMINATION LEVEL:	PU: Public
FILENAME:	FIBREGY_D6.3
STATUS:	First version

Authoring & Review

PREPARED / REVIEWED BY				
Name	Role	Partner	Date	Comments
Mário Moutinho	Contributor	INEGI	13/07/2023	
João Cardoso	Contributor	INEGI	31/07/2023	
Rúben Ferreira	Contributor	INEGI	31/07/2023	
Cristobal Garcia Pariente	Contributor	TSI	20/07/2023	Chapter 10 and 11

This project has received funding from the European Union's Horizon 2020 research and innovation programme under grant agreement No 952966.

EXECUTIVE SUMMARY

This report details the design work done in task 6.2.1 ("TIDETEC's turnable turbine housing"), where a turnable turbine housing was manufactured at INEGI's premisses using FRP materials and the automated fibre placement (AFP) process.

Throughout this report, the process of re-engineering and re-designing of the turnable turbine housing unit will be detailed, as well as the process definition, optimization, and final manufacturing. After manufacturing, the resulting structure was tested and validated using vibration and impact assessments performed by TSI.

This work comes as a continuation of the work done in D4.2, which ensured the viability of the composite structure with a finite element analysis. Since then, the design of the FRP turbine housing has been adjusted based on the needs of both TIDETEC and the manufacturer (INEGI) in order to ensure its manufacturability. This also included the design and selection of the most appropriate connections and the design of the mandrel where the fibres were laid up. The final housing will be able to fit the existing turbine model, consequently resulting in one of the two large-scale demonstrators for the FIBREGY project.

Although some noteworthy changes were made from the planned scope, being the most notorious the change from the filament winding process to the automated fibre placement process, the reasons behind these modifications are well explained through this document and were always made with the purpose of ultimately lead to a significant increase of maturity in the technologies with most added value for the offshore industry, namely relying on an automated and reliable process that can be agilely industrialized.

This document is an important contribution to Milestone 11 – "Turnable turbine housing demonstrator", demonstrating the capabilities of automated processes for the manufacturing of these large offshore structures, as well as the necessary steps to guarantee its manufacturability.

This project has received funding from the European Union's Horizon 2020 research and innovation programme under grant agreement No 952966.

TABLE OF CONTENTS

This project has received funding from the European Union's Horizon 2020 research and innovation programme under grant agreement No 952966.

LIST OF FIGURES

This project has received funding from the European Union's Horizon 2020 research and innovation programme under grant agreement No 952966.

This project has received funding from the European Union's Horizon 2020 research and innovation programme under grant agreement No 952966.

LIST OF TABLES

This project has received funding from the European Union's Horizon 2020 research and innovation programme under grant agreement No 952966.

LIST OF ACRONYMS

Acronym	Meaning
NDT	Non-Destructive Test
FFT	Fast Fourier Transform
FRP	Fibre Reinforced Polymer
KPI	Key Performance Indicator
ROI	Return of investment
SHM	Structural Health Monitoring
VSHM	Vibration based Structural Health Monitoring

This project has received funding from the European Union's Horizon 2020 research and innovation programme under grant agreement No 952966.

1. CONTEXTUALIZATION

The turbine housing demonstrator for the FIBREGY project can be traced back to the idea from TIDETEC to build an innovative and cost-effective tidal turbine [1] (Figure 1), which was originally designed to be manufactured using mainly steel materials. Within the scope of the FIBREGY project, it is aimed to transition this to a composition construction, having a significant impact on its weight reduction, which directly impacts the turbine's Operational Expenditure (OpEx). The use of lightweight materials and advanced design is expected to considerably reduce the housing's weight, which will enhance the turbine's turning operation, optimizing energy capture from tides and reducing mechanical strain. The lighter housing also translates to lower maintenance costs for the bearing system, promoting the long-term sustainability and economic viability of the tidal energy system.

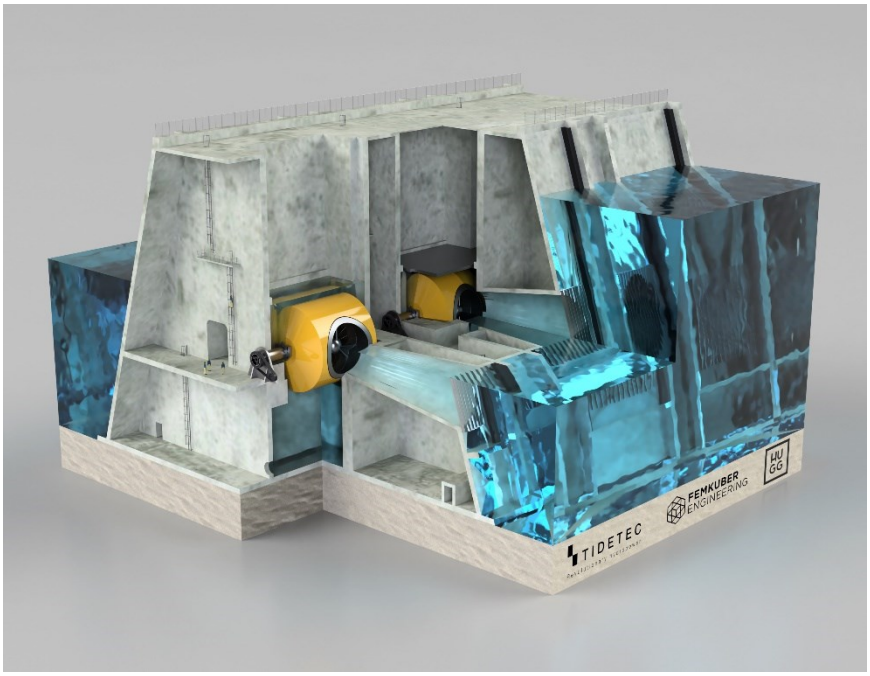

Figure 1 – Tidetec's turbine solution [1]

However, the transition to composite construction posed significant challenges. It became evident that attempting to replicate the steel construction with composites directly would not yield efficient results, if feasible at all. Therefore, the FIBREGY team saw this as an opportunity for innovation, and as will be seen in this document, several manufacturing processes and design strategies were considered along an extensive iterative process, in order to capitalize on the unique advantages of composites.

This project has received funding from the European Union's Horizon 2020 research and innovation programme under grant agreement No 952966.

2. PROCESS DEFINITION

The first step of the development of the composite design for the turbine housing was the definition of its manufacturing process, as it will directly impose design limitations and provide some orientations for designing an efficient structure while being manufacturable using accessible means and equipment. Therefore, despite having previously planned to use the Filament Winding process, the decision to employ Automated Fibre Placement (AFP) over Filament Winding was carefully considered and justified by several key factors. Automated Fibre Placement, a cutting-edge manufacturing technique, was primarily chosen due to its ability to offer superior control, precision, and efficiency in constructing the turbine housing demonstrator.

AFP enables the strategic placement of continuous fibres with high accuracy and minimal waste, ensuring a robust and optimized material distribution throughout the structure. This precision is crucial for achieving the desired mechanical properties and structural integrity required for the turbine housing. Additionally, AFP allows for the integration of complex geometries and curvatures (it is ideal for making cylindrical and/or hemispheric components), making it well-suited for the intricate design requirements of the turbine housing and other OWTPs.

Compared to Filament Winding, which involves the winding of pre-impregnated continuous fibres onto a rotating mandrel, AFP streamlines the production process and significantly reduces the manufacturing time, thus leading to increased cost-effectiveness and faster production cycles. Moreover, the automated nature of the AFP process reduces manual labour, minimizing the risk of human errors and ensuring consistent quality in the final product. Considering these factors, the selection of Automated Fibre Placement as the preferred manufacturing method for the turbine housing demonstrator in the FIBREGY project proves to be a well-founded and advantageous choice that aligns with the project's objectives of developing an innovative, high-performance, and cost-efficient component.

Moreover, when considering INEGI's capabilities, using AFP has allowed for the demonstration and validation of their new AFP equipment (Figure 2), which also allows for the production of bigger parts when compared to their filament winder (Figure 3). Its main disadvantage is the higher material cost (which is towpreg – pre-impregnated with resin – instead of dry fibres) and then the need for cold storage of the material in a freezer.

This project has received funding from the European Union's Horizon 2020 research and innovation programme under grant agreement No 952966.

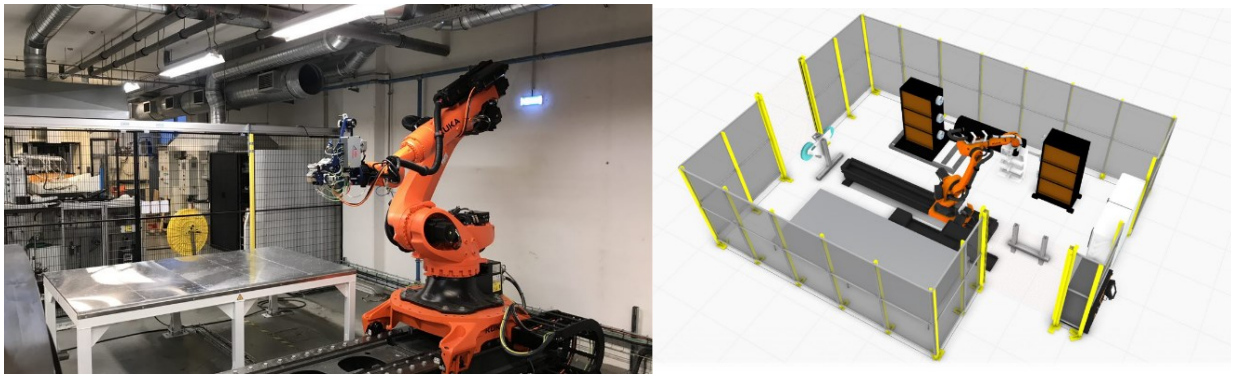

Figure 2 – AFP machine

Figure 3 – Pultrex Modwind 1S 6NC

The main technical characteristics of the AFP equipment are:

- Fibre configuration: 5-25mm
- Cut and feed repeatability: +-0,5mm at 300mm/s
- Compaction force range: 0 to 350 N
- Maximum layup speed 250 mm/s
- Thermoplastics and Thermosets

This project has received funding from the European Union's Horizon 2020 research and innovation programme under grant agreement No 952966.

3. DESIGN FOR MANUFACTURING (DfM)

Although the geometry of the turbine housing was already detailed in D4.2 – "Turnable Tidal Turbine design for FRP adaption of components" and D4.5 – "Turnable Tidal Turbine demonstrator design for its construction", the process of design for manufacturing has matured further in order to adjust to the defined process as well to ensure the manufacturability of the mandrel, which was seen to be challenging. Thus, the main objective was to ensure that the final product can be efficiently and economically produced without sacrificing its functionality or performance.

The process of achieving an optimized design for manufacturing the turbine housing demonstrator in the FIBREGY project involved multiple iterative stages. The initial iteration (Figure 4) consisted of a composite design provided by TSI, which exhibited significant improvements compared to the original steel design. However, certain challenges persisted, particularly related to sharp angles and assembly issues. Subsequently, the second iteration focused on resolving these issues while maintaining a strong emphasis on manufacturability.

Figure 4 – DfM (1st iteration)

Cons:

- Sharp angles 1 through 5;
- Assembly with nut and bolts between 3 and 4 is impossible to reach;
- Joining 3 and 4 with adhesive defeats the purpose of turbine accessibility for maintenance;
- Requires use of 2 mandrels.

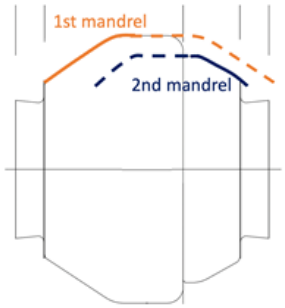

Figure 5 – Required usage of two mandrels

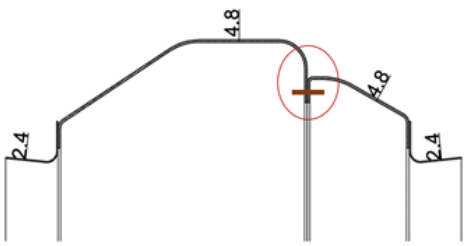

Figure 6 – Impossibility of accessing the bolted connection

This project has received funding from the European Union's Horizon 2020 research and innovation programme under grant agreement No 952966.

During the second iteration (Figure 7), considerable effort was dedicated to identifying and rectifying manufacturing challenges. Despite significant progress, further refinement was necessary to meet project requirements.

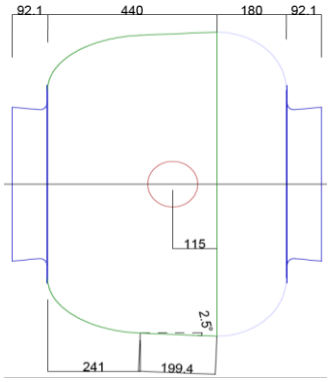

Figure 7 – DfM (2nd iteration)

Pros:

- Smoother angles;
- Only requires one steel mandrel;
- Has demoulding angle which facilitates manufacturing.

Cons:

- Studs are not necessary;
- Domes' geometry undefined for manufacturability.

Given the critical role of the mandrel in the manufacturing process - serving as the essential mold onto which the towpreg (fibre pre-impregnated with resin) is laid - particular attention was directed towards ensuring its manufacturability. The complexities arising from the domes, or end caps, presented risks of slippage, twisting, or other defects during fibre placement.

To address these challenges, a comprehensive evaluation of various shapes was undertaken, aiming to strike a balance between the draft angle required for easy demolding and the optimal angle and shape for precise towpreg placement. Extensive fibre placement simulations were performed to inform the decision-making process, seeking an ideal configuration that could seamlessly integrate manufacturability and design integrity.

At first, preference was given to components that can be bought out-of-the-shelf, hence it was reviewed the different ASME standard dish heads, detailed in Figure 8, and that would need to be welded to a middle section of either a tube (in case of the same dish head on both sides) or a cone (in case of different dish head on each end). As will be seen, the available outer diameters for the different dish head types would implicate that if the middle were a cone the demoulding angle would be too large and could even hinder the manufacturability of the housing.

This project has received funding from the European Union's Horizon 2020 research and innovation programme under grant agreement No 952966.

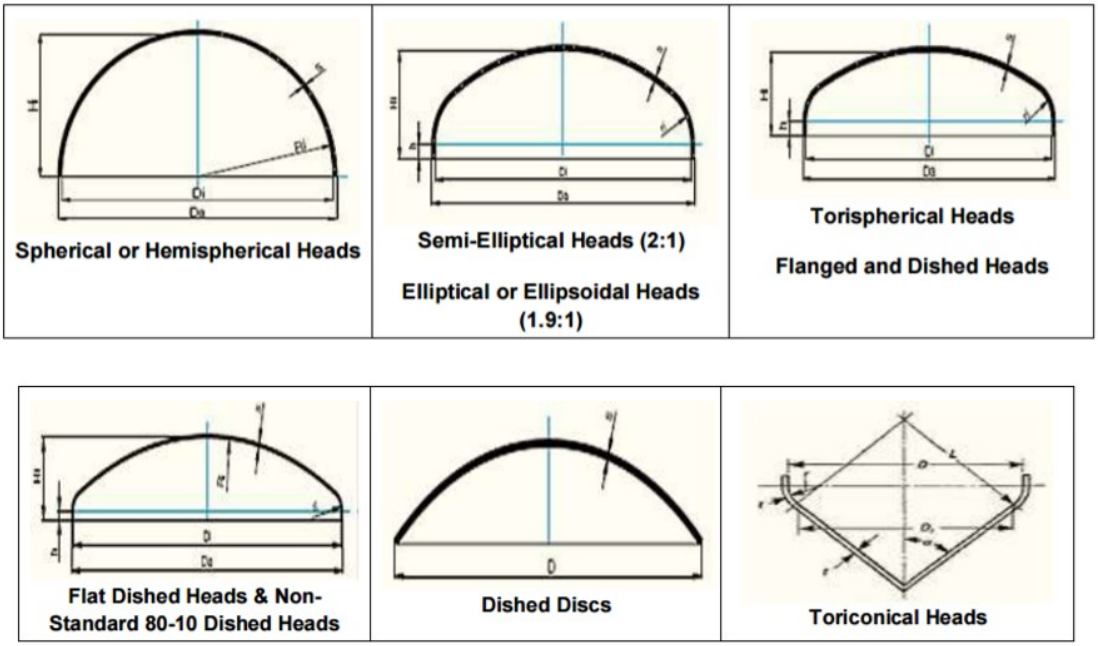

Figure 8 – Standard or out-of-the-shelf available dish heads for integration into the housing mould

Some of the simulations using different end cap geometries can be seen in the following images.

Low pressure Dish Head

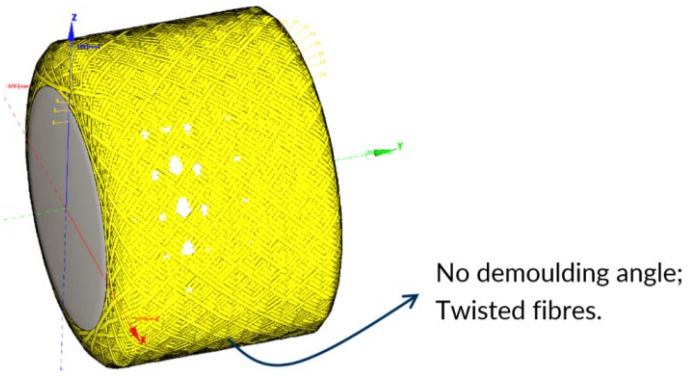

Figure 9 – Low-pressure Dish Head

Pros:

- Cheaper and easier to manufacture the mandrel.

Cons:

- Not windable in the software if considering demoulding angle;
- High likelihood of twisted and/or breakage of tows.

This project has received funding from the European Union's Horizon 2020 research and innovation programme under grant agreement No 952966.

Torispherical Dish Head Type Klopper (with flange) - DIN28011

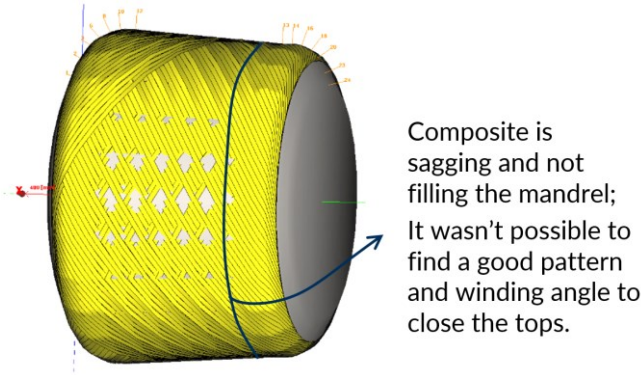

Figure 10 – Torispherical Dish Head Type Klopper (with flange)

Pros:

- Easier to manufacture mandrel.

Cons:

- Not feasible in winding software.

Angle: 3,82° → too high
Height: 91 and 104 mm

Torispherical Dish Head Type Klopper (without flange) - DIN28011

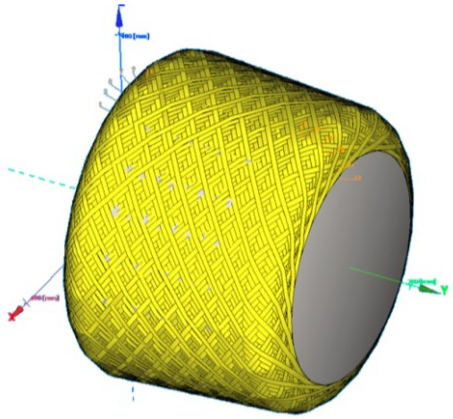

Figure 11 – Torispherical Dish Head Type Klopper (without flange)

Pros:

- Windable but with limitations.

Cons:

- Harder to manufacture mandrel because of the peripheral weld near the radius.

Angle: 3,37°
Height: 91 and 104 mm

The culmination of these investigations led to a significant realization: a custom shape (Figure 12) was imperative for this project. The resulting custom shape featured a draft angle of approximately 1,5 degrees, fulfilling the essential criterion for easy demolding while providing an ideal foundation for accurate and defect-free towpreg placement, as supported by the simulations. The proposed profile is a semi-sphere, which turns out to not deviate much from the initially presented design for the Turnable Tidal Turbine profile. The resulting production drawings for the housing mould can be seen in Figure 12 through.

This project has received funding from the European Union's Horizon 2020 research and innovation programme under grant agreement No 952966.

Spherical Dish Head - Custom

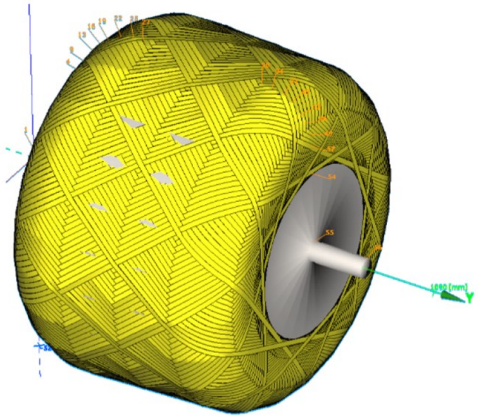

Figure 12 – Spherical Dish Head - Custom

Pros:

- Smoother angles (closer to TSI design shape);
- No twisting of fibres;
- Good demoulding angle.

Cons:

- More expensive manufacture.

Angle: 1,55°
Height: 129 and 169 mm

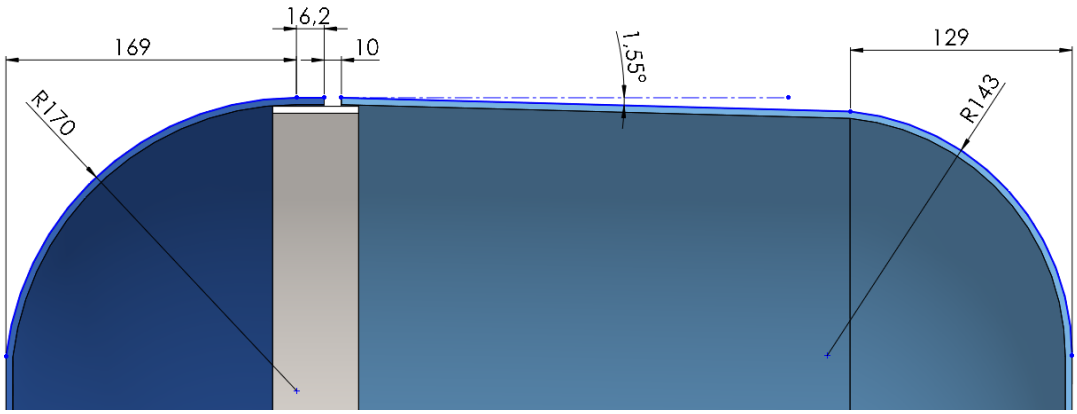

Figure 13 – Detailed dimensions of the custom mandrel

a)

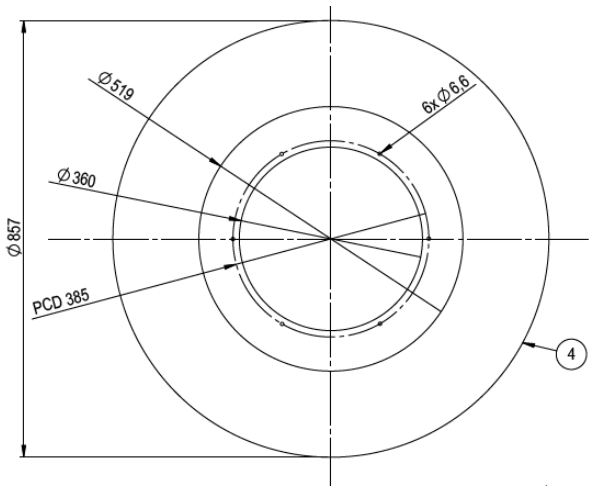

b)

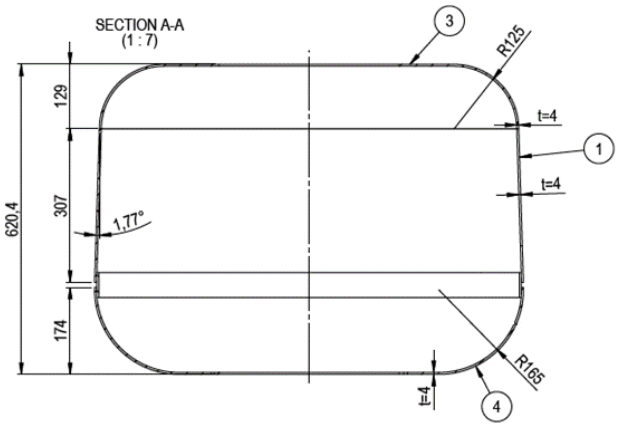

This project has received funding from the European Union's Horizon 2020 research and innovation programme under grant agreement No 952966.

c)

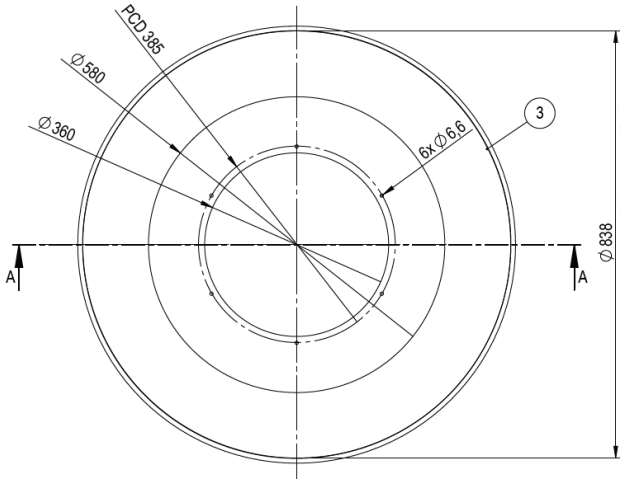

Figure 14 – Production drawings for the Turnable Tidal Turbine housing mould

This final design was obtained through structural analysis of the Tidal Turbine assembly in the different modes of operation, and also combined with qualitative measures regarding manufacturing and assembly restrictions, such as:

- A housing that can be produced with a minimal number of auxiliary components, ideally requiring only one modular mould for the entire housing;
- A housing that can be opened up for turbine maintenance, requiring easy assembly and disassembly via external connections with nuts and bolts;
- A housing with a rounded revolution profile with a high radius instead of cones with high slope, sharp angle transitions or 0/90° angles;
- The direction of the demoulding part should not feature fully convex or concave shapes otherwise it will lock the part in the mould. A demoulding angle is optional but a helpful feature;
- The structural analysis should foresee that a winded part will have a higher thickness on the extremities or the nearest part to the axis of revolution;

However, this designed profile, though ideal considering FRP, was proven hard to achieve with a corresponding mould manufactured in steel. The manufacturing process for FRP works best with steel or aluminium moulds, and for this dimension of outermost diameter 867 mm, the manufacturing of the mould is limited to very specialized stainless-steel conformation and welding processes. Fortunately, a suitable manufacturer was identified, capable of accommodating this unique requirement.

Furthermore, the total length of the housing was designed to be larger than that of the TSI design because it is expected different overall thickness at the bottleneck of the housing, but also because the housing will be made of two halves that will need trimming and cutting requiring

This project has received funding from the European Union's Horizon 2020 research and innovation programme under grant agreement No 952966.

extra through away material. Overall, it was given 10 mm extra as leeway to compensate eventual fluctuations of total length for the obtained housing.

Different modular building strategies were considered in order to allow for the removal of the part from the mandrel as well as the access to the turbine inside the housing. From the Figure 15 it can be depicted that strategy B was followed, having a transversal cut section that allows easy removal of both sides.

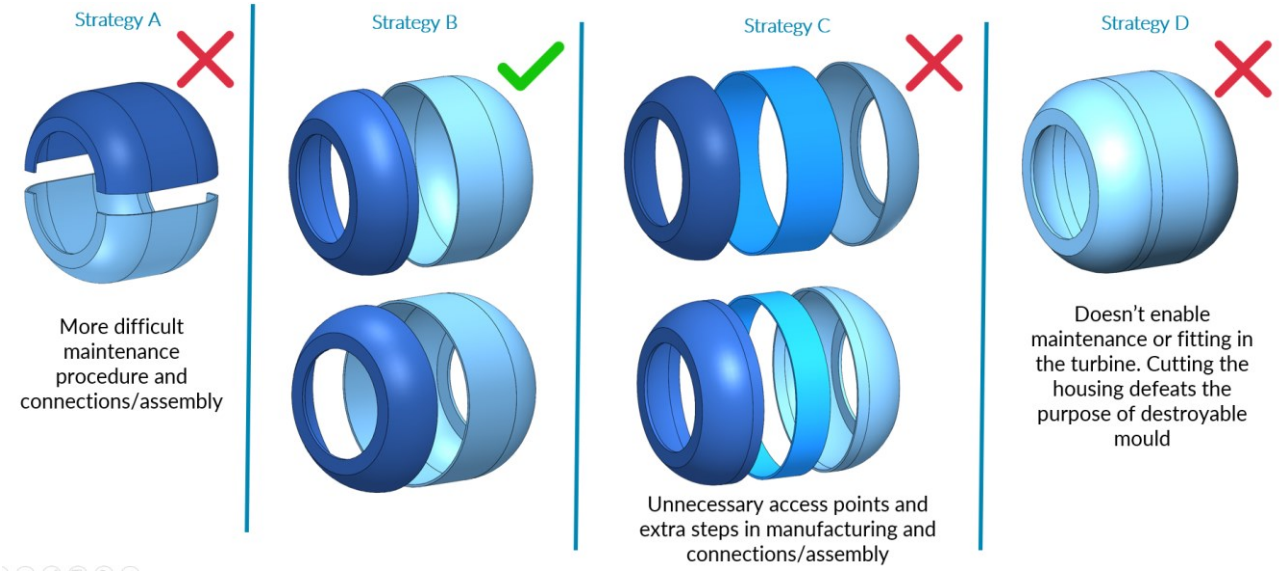

Figure 15 – Modular building strategies

The resulting two parts were named main body and aft cover, and the connection between them was designed as an external flange, bonded to the composite and then bolting the two flanges together. It was decided that the aft and forward fairings will be bonded to the cured housing. Some of the evaluated connection possibilities, as well as the resulting process chain, are illustrated in Figure 16.

This project has received funding from the European Union's Horizon 2020 research and innovation programme under grant agreement No 952966.

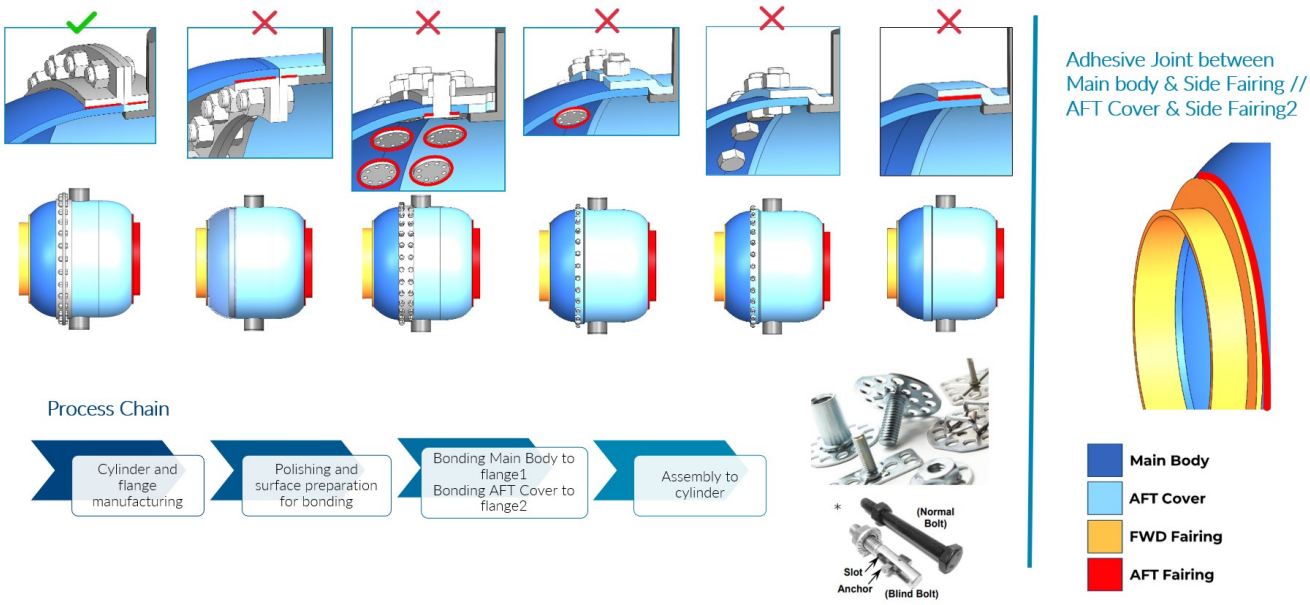

Figure 16 – Selection of connections and resulting process chain.

And the resulting assembly plan is illustrated in Figure 17.

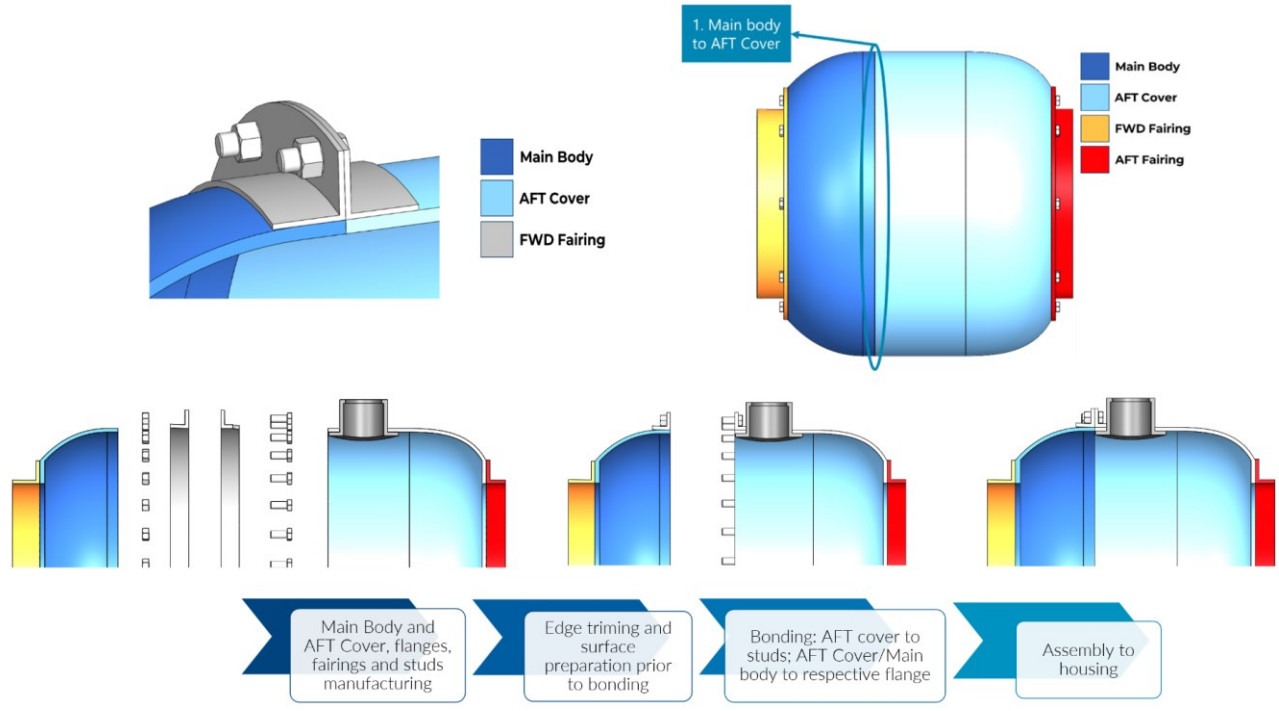

Figure 17 – Final assembly plan

The calculation of the minimal required diameter of the shafts is influenced by multiple factors, including the self-weight of the mandrel, by the pressure that the compaction roller of the AFP

This project has received funding from the European Union's Horizon 2020 research and innovation programme under grant agreement No 952966.

machine does onto the mandrel and the distance between the supports. Several numerical Simulations were also conducted to investigate the effect of varying shaft diameter on the maximum deflection expected. The minimum shaft diameter required to maintain a maximum allowable deflection of 2 mm was determined considering a shaft diameter of 50 mm, decided considering the results illustrated in Table 1. This deflection will also influence the position of the compaction roller leading to incorrect tape deposition, and it is ensured that the shaft has sufficient length on each side to allow all the necessary robot movements without interferences.

Table 1 – Maximum deflection of the shaft for different diameters.

Ø Shaft [mm]	Maximum deflection of shaft [mm]		Weight of shaft tips[kg]
	Self Weight	Self Weight+ Tension of 10 fibres (80N*10 or 342,616Nm)	
45	1,642	3,488	25,8
50	1,127	2,346	31,5
55	0,809	1,651	37,9

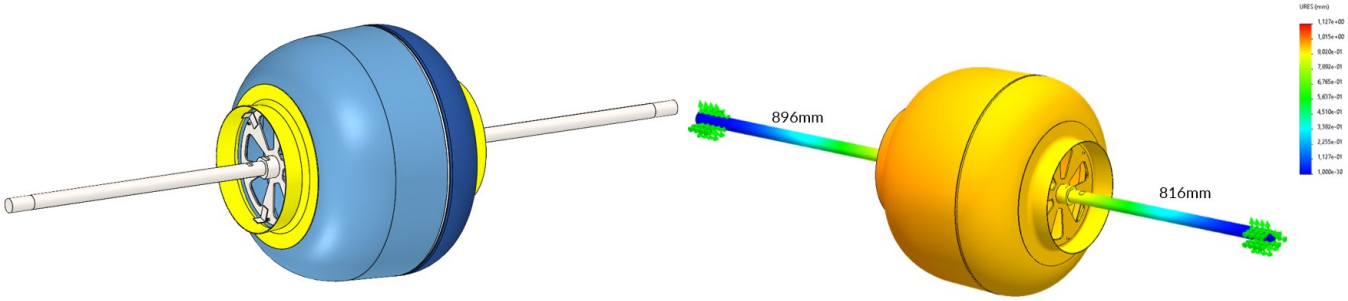

Figure 18 – Deflection simulation

This project has received funding from the European Union's Horizon 2020 research and innovation programme under grant agreement No 952966.

And the assembly mockups of the mandrel and the resulting composite can be seen in Figure 19. The technical drawing for manufacturing the mandrel is in Figure 20.

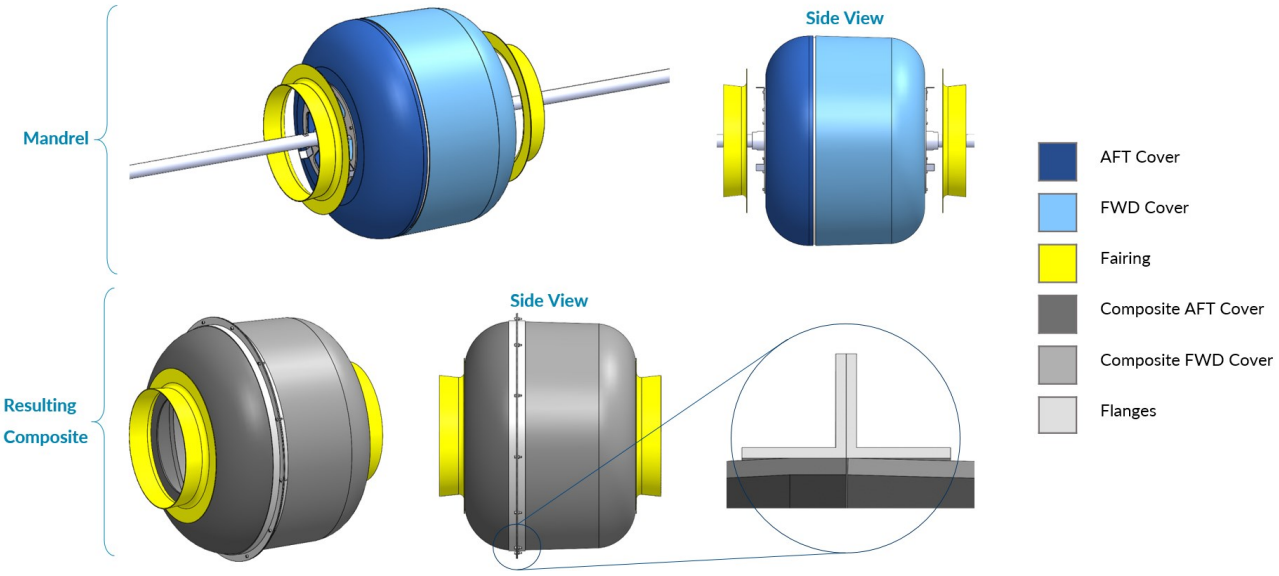

Figure 19 – Mockups of the mandrel and the resulting composite.

This project has received funding from the European Union's Horizon 2020 research and innovation programme under grant agreement No 952966.

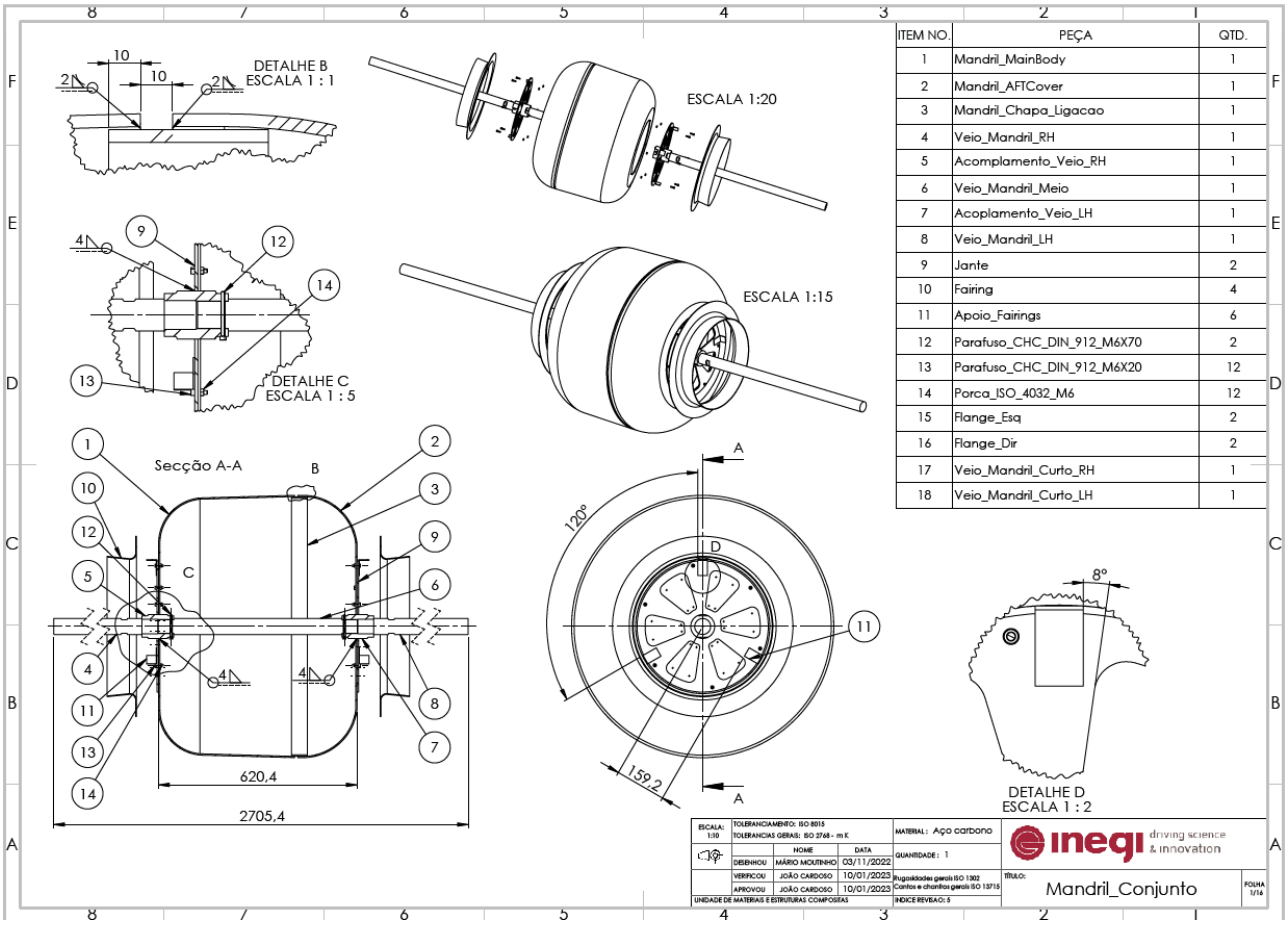

ITEM NO.	PEÇA	QTD.
1	Mandril_MainBody	1
2	Mandril_AFTCover	1
3	Mandril_Chapa_Ligacao	1
4	Veio_Mandril_RH	1
5	Acomplamento_Veio_RH	1
6	Veio_Mandril_Meio	1
7	Acoplamento_Veio_LH	1
8	Veio_Mandril_LH	1
9	Jante	2
10	Fairing	4
11	Apoio_Fairings	6
12	Parafuso_CHC_DIN_912_M6X70	2
13	Parafuso_CHC_DIN_912_M6X20	12
14	Porca_ISO_4032_M6	12
15	Flange_Esq	2
16	Flange_Dir	2
17	Veio_Mandril_Curto_RH	1
18	Veio_Mandril_Curto_LH	1

Figure 20 – Technical drawing for manufacturing the mandrel.

This project has received funding from the European Union's Horizon 2020 research and innovation programme under grant agreement No 952966.

4. MANDREL PREPARATION

Upon receiving the mould, a verification of the most critical dimensions was conducted to ensure they aligned with the drawing specifications. Specifically, the outermost diameters of ⌀ 857 mm and ⌀ 838 mm, at the edge of the dish heads were calculated by measuring the perimeter. The total length of the mould 620.4 mm, was also verified. Furthermore, a thorough inspection was carried out to identify any concave or convex areas that might pose complications during the demoulding process.

Unfortunately, it was found that the mandrel had some warping and sinking regions caused by the welding process, and this would result in being impossible to demould the part, so an overall correction of the surface had to be made by applying polyester putty all over the mould and then priming the geometry in a lathe, thus ensuring that there is a uniform draft angle. Afterwards, to prevent the composite from reacting with the putty during the cure, the mandrel was painted with polyester paint also giving better protection against scratching and chemical cleaning. The corrected mandrel can be seen in Figure 22.

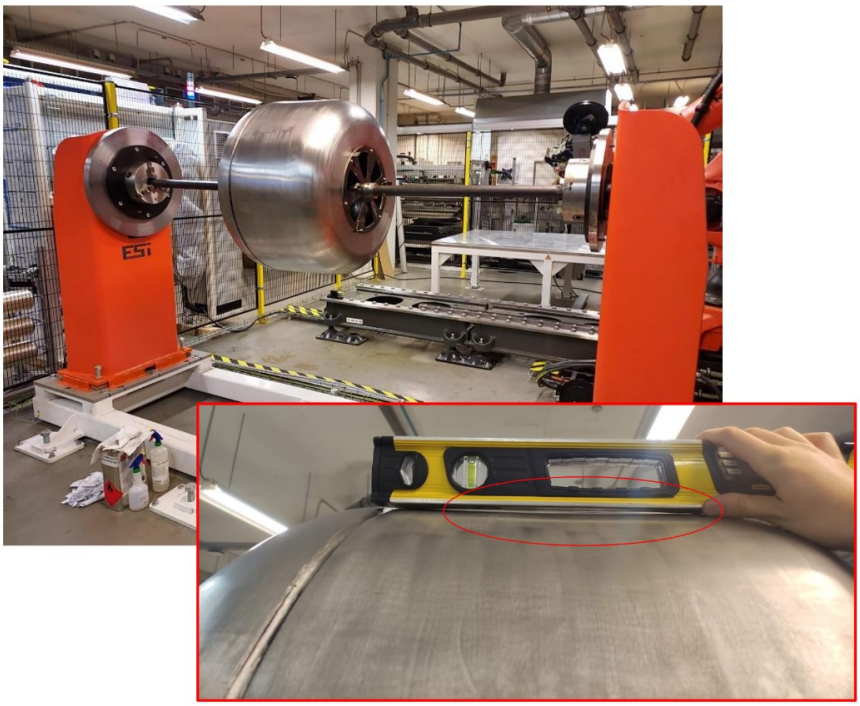

Figure 21 – Negative draft angle due to sinking/warping

This project has received funding from the European Union's Horizon 2020 research and innovation programme under grant agreement No 952966.

Figure 22 – Good draft angle after correction

Once the mandrel is cleared for usage, the shafts and rims were assembled onto the mandrel using nut and bolt connections, as illustrated in Figure 23. Subsequently, the assembly was mounted onto the robot supports as depicted in Figure 24. It was crucial to pay special attention to securely fastening the chuck to prevent any sliding of the shafts during rotation. Additionally, it was essential to ensure that the distance between the centre of the chuck and the beginning of the mandrel matches the specified value in the program.

Figure 23 – Shaft and rims for connection between mandrel and robot supports

This project has received funding from the European Union's Horizon 2020 research and innovation programme under grant agreement No 952966.

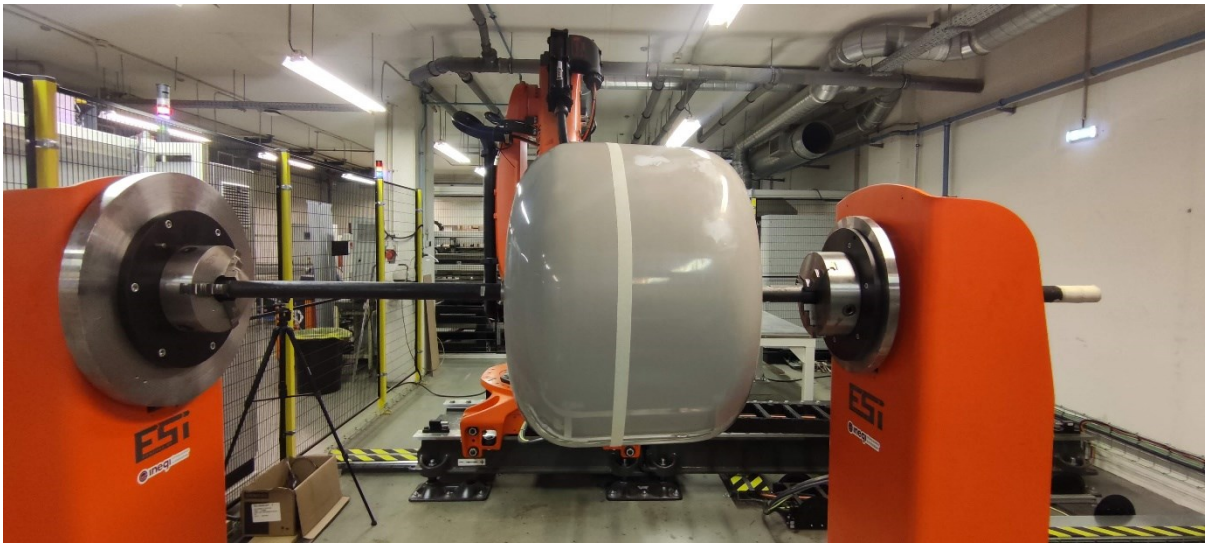

Figure 24 – Assembly of the mandrel on the robot supports

The deposition area limits on the mandrel are marked on the mandrel using Flashbreaker tape or paper tape to create a space for the vacuum bagging sealant tape to adhere during the final curing stage. Since the surface of the mold is painted, a mould cleaner liquid was not used; instead, isopropyl alcohol was applied to clean the surface. Following the cleaning process, four layers of liquid demoulding agent Frekote 770-NC are applied to the deposition area. Each layer is spaced 15 minutes apart. Finally, three layers of demoulding wax are applied, with a 15-minute interval between each layer, as illustrated in Figure 25. In this figure, it is also possible to see some degradation of the mould surface (paint) after undergoing a cure cycle.

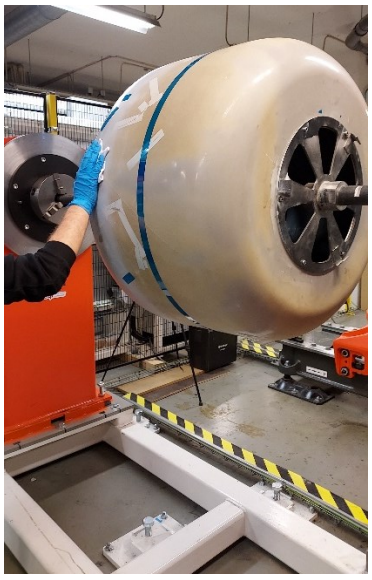

Figure 25 – Priming the surface of the mould with demoulding agents on the deposition area

This project has received funding from the European Union's Horizon 2020 research and innovation programme under grant agreement No 952966.

5. MANUFACTURING TRIALS

For the manufacturing trials, it is first necessary to build up the program for the robot to be able to layup the tapes automatically. The AFP head mounted on the robot was made by AddComposites and their tape layup planner is the AddPath plugin for the Rhinoceros 3D Cad program.

To start off, it is necessary to import the workspace cad with the respective robot cell. Then, it is imported the file with the geometry of the mandrel in IGES format and all the external surfaces are selected as Mold Geometries. In this first step, it is also important to select the Mold Reference which refers to the centre point of the beginning of the shaft. The Mold Reference is then aligned with the centre of the chuck which is referred to as Base axis. By adjusting the X axis alignment, it is changed the position of the beginning of the mold and thus this parameter has to be well refined. In summary, this first step is displayed on the tab displayed in the following Figure 26.

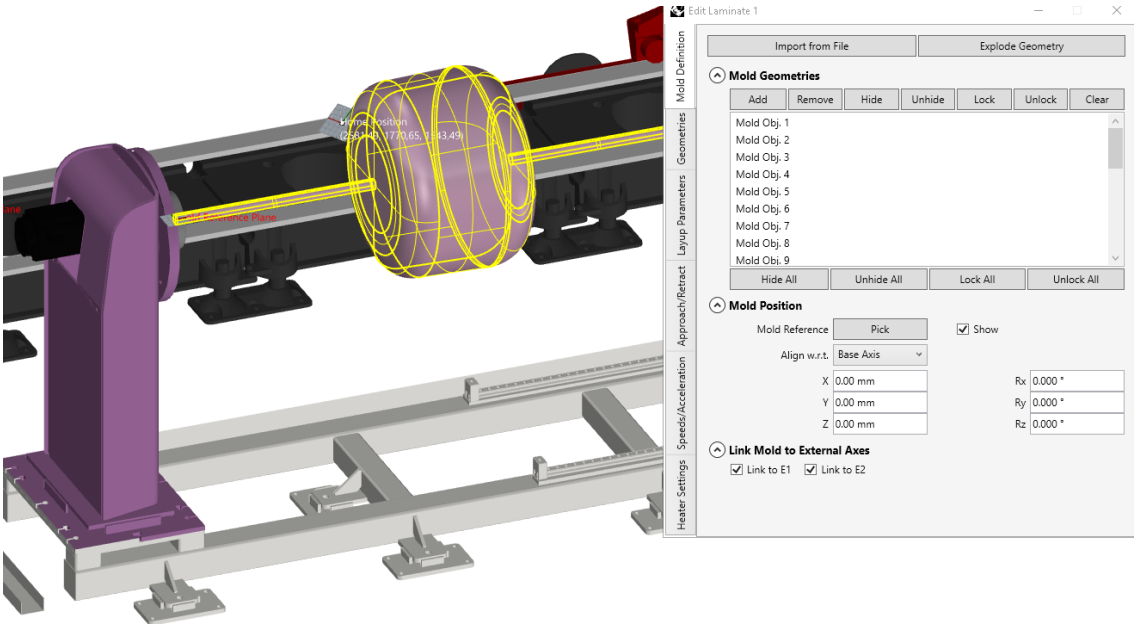

Figure 26 – Mold definition and position in the Rhinoceros 3D using AddPath plugin

The linking of the axis E1, corresponding to the carriage system of the robot, and E2, corresponding to the rotation of the chuck in the robot supports, is also necessary to enable a full range of the movements of the robot.

The second step that can be followed in Figure 27, involves defining the planner mode which is Discontinuous Winding and respective Planning Area. The Planning Area requires defining several key parameters. These include the Layup Area, which designates the region where the tapes will be placed, the Boundary Area which specifies where the tapes should not extend beyond, the Periphery Edge representing the edge used for the mandrel's revolution reference,

This project has received funding from the European Union's Horizon 2020 research and innovation programme under grant agreement No 952966.

and the Zero Direction with the Direction plane. The Direction plane is set at 0° along the axis direction and 90° in a perpendicular direction to the axis. It is crucial to ensure that the direction of tape stacking is correct, as an inward-facing arrow could result in the robot head colliding with mold. Additionally, the winding priority can be established by choosing either “Prioritize gaps” or “Prioritize orientation”. However, in this particular case, the choice between the two does not significantly affect the planning process of the tapes.

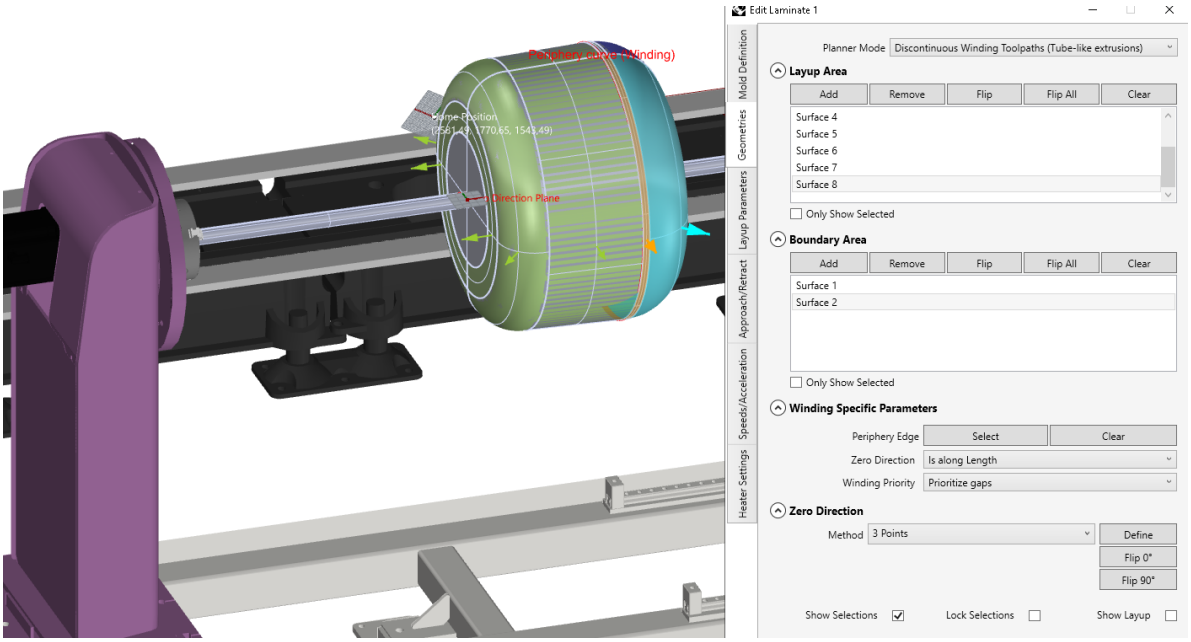

Figure 27 – Planner mode and Layup area definition

The end step for this plugin can be followed in Figure 28, and involves defining the Layup Parameters. Here it is specified the material being used, namely the Areal Density (324 gsm), Tow Width (6.35 mm) and Tow Thickness (0.32 mm), and the ply angle definition.

The diameter achieved with laid-out tapes near the shafts, specifically at the extremity of the housing, is determined by the ply angle and the layup area. A higher ply angle results in a larger aperture, whereas a lower ply angle restricts the tapes within the layup area. Considering that the roller is wider than the tape and constrained to the edge of the rims, an optimal angle of 33° was chosen. At this angle, the edge of the roller nearly touches the edge of the rim, ensuring that the diameter of the aperture at the extremity is minimized as much as possible.

Furthermore, the planning of the tapes is only possible by relaxing the planner tolerances to a Curve Offset of Marching Distance equal to 1 mm. The Runaway length was defined to be equal to 1 mm to enable automatic compaction and tape feed at the beginning of each tape.

This project has received funding from the European Union's Horizon 2020 research and innovation programme under grant agreement No 952966.

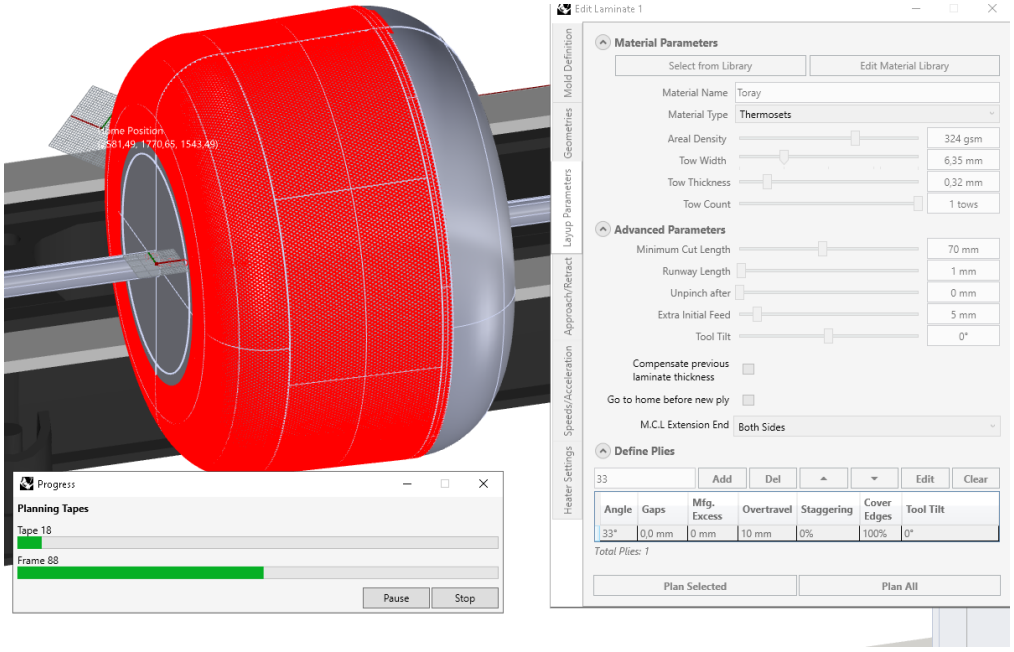

Figure 28 – Layup parameters

The angle for the ply could also be lower if it was adjusted the layup area so that the roller would end the ply close to the rim. However, 33° is much closer to the optimal winding angle for standard parts and with the 33° option, the robot is continuously laying a tape on the return to the initial position of the next tape so the winding is twice as fast.

The heating lamp that turns on during the deposition was set to 60% which generates roughly 50°C to 60°C (Figure 29) on the area of the mandrel closest to the lamp. This temperature enabled optimal adhesion and conformation of the tapes to mandrel.

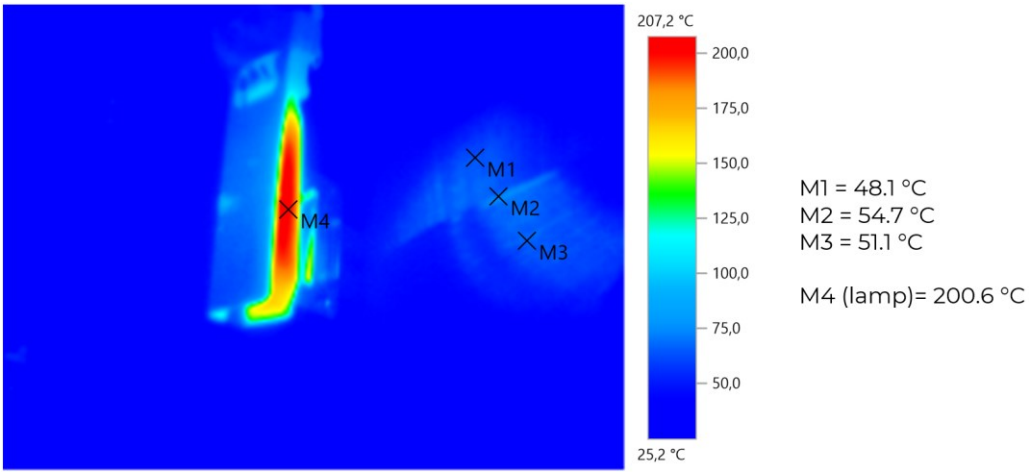

Figure 29 – Thermography near the lamp

The resulting planning of the tapes resulted in 358 tapes per layer with 1674 m per tape on one side and 1013 m on the other.

This project has received funding from the European Union's Horizon 2020 research and innovation programme under grant agreement No 952966.

An initial test of the deposition of the tapes was carried out, of which the result is displayed on the following Figure 30. It was found that it was necessary some adjustments to the CAD of the mandrel to increase the pressure of the roller and also some minor adjustments to the shape of the profile of the dish head. The ideal situation is when the tapes are laid out without gaps and without overlapping. Another possible adjustment could be to modify the width of the tapes to force the position of the tape. As in this case there were some clear issues with the variation of the pressure of the roller, only the CAD of the mandrel was modified.

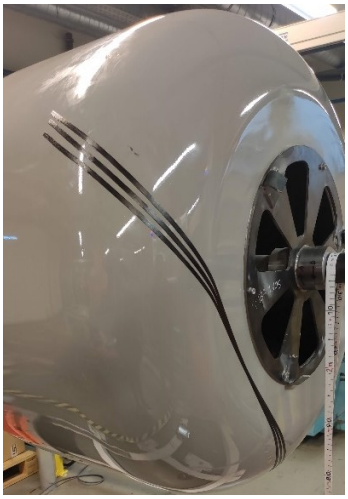

Figure 30 – Initial manufacturing trials

Also, it was found that the coordinates for the Base axis or centre of the chuck were different from the robot definition and program definition, and the only reason the program still worked was that this base is called in the program by its number ID and not the coordinates in itself. As such, there was present overpressure on the return and almost no pressure on the roller from the start to the middle of the tape. After changing this value, it was now found uniform pressure of the roller and set to 150 to 160MPa.

There was also present an issue with the overload of the feeding motor or jamming of the head at the start of each tape. After analysing the feeding mechanism, it was discovered that when the robot is turning backwards at the middle of the tape its velocity is instantaneously zero and before and after that the head deaccelerates a bit. The feeding however is continuous and as it doesn't keep up with the actual travelled distance it runs inside the feeding rolls on itself clogging the machine. The solution found and implemented was to turn off feeding after the initial runaway and approach path, being the tows feed through pulling and not through the feeding motors.

The program planned can also be simulated on the Rhino 3D, to check for collisions of the robot in the cell before actually uploading it onto the robot. After validating everything, with all the optimal and necessary parameters the final program can be generated using a custom post-processor file.

This project has received funding from the European Union's Horizon 2020 research and innovation programme under grant agreement No 952966.

6. MANUFACTURING

After the successful manufacturing trials, everything was set up to manufacture the large-scale demonstrator. To do so, the head uses a spool holder on a shaft with a tensioning motor at the foremost part of the head. It is on this shaft where the material is held on a Hafner tape reel with the designation Flange BSH 315. Unfortunately, this head only supports material with this type of system where the material is winded unilaterally on this type of tape reel and not helically spooled or with slit tapes as one would normally find in other AFP machines.

To find a material to fit the machine, there is the option of resorting to custom slit tapes with specific or approximate dimensions to the original tape reel format or the option of taking helical AFP spools that would need to be respooled to the tape reels. AddComposite, despite envisioning the system with these tape reels and selling empty tape reels, doesn't supply material.

As the AFP spools could also be used in other winding systems at INEGI, such as the upcoming Towpreg winding, this was the chosen option. In the following Figure 31, it can be found an initial jig that was set up for the respooling of the AFP spools. At the upstream on the top right corner of the picture there is a tensioning machine that was otherwise being used in a custom prepreg machine, at the middle of the jig there are some guiding rollers, and at the downstream there is the original robot tape reel that is being rotated by the filament winding machine.

Figure 31 – Respooling jig of the AFP spools onto the Hafner tape reels

These tape reels, as they were being respooled and unspooled, needed also occasional cleaning to prevent fibre strands from pulling while feeding during the manufacturing of the housing.

As the AFP material is stored frozen, there must be caution to store it in sealed bags with silica bags inside to prevent humidity from damaging the material. Before use and opening the sealed

This project has received funding from the European Union's Horizon 2020 research and innovation programme under grant agreement No 952966.

bags, the material should be left at room temperature for about half an hour for the tape reels and one hour for the AFP spools, so that there isn't condensation forming on the material and damaging it.

The first layer required slower laying tape speeds to ensure better adhesion to the paint of the mandrel. From the middle of the first layer onwards, the deposition of the tapes is already happening on top of previous tapes so it can be used at the maximum speed. As each layer is locally taped criss-crossing at angles of +/−33°, the actual thickness of one layer is estimated to equal twice the thickness of the tow.

Furthermore, an error arose during the initial layer where the feeding motor would overload after completing the deposition of each tape. After closely observing the process, it was determined that certain areas had the feed running slightly faster than the movement of the head. To address this problem, the pinch mechanism, which is the roller responsible for pressing the tape against the feeder roller, was deactivated during deposition. By doing so, the deposition process relied on pulling the tape rather than relying solely on the feeding mechanism, resolving the issue.

After some tapes, the machine's performance started to degrade and it could even appear again a warning of the feed motor overload. At this point, it was established routine cleaning of the head every 50 layers. It was thoroughly cleaned the feeding roller, the end shut part, the guiding rollers, and the cutting mechanism of the tapes. For this, it was used acetone, since it was found to be more effective at removing the resin of these parts where the leftover resin from the tapes would start pulling fibre strands and thus clogging the machine. Before rerunning the tows on these parts, it was dried out the acetone with a clean cloth so that it wouldn't damage the tows.

Because of the weight of the mandrel, it was necessary to refasten the shafts to the chuck as they tend to lose their grip with the rotation and force of the compaction roller on it. Without this step, it was noticeable small gaps started to appear between tows and with growing gap width.

In the following set of photos in Figure 32, it is possible to verify the progression of the deposition of the tapes onto the mandrel.

This project has received funding from the European Union's Horizon 2020 research and innovation programme under grant agreement No 952966.

Figure 32 – Production sequence of timelapse photos for the first layer

This project has received funding from the European Union's Horizon 2020 research and innovation programme under grant agreement No 952966.

The angle of the head in relation to the perpendicular plane to the mandrel axis is defined by the bias angle. The angle of the tape is given by the rotation of the mandrel in relation to the linear movement of the head in the X axis. The head twists and turns but its position in the Z axis is fixed by the bias angle, while the Y coordinate is dictated by the mandrel geometry.

Figure 33 – Manufacturing of the main body

This angle is important because if equal to -90°, the robot collides with the shaft and if it reaches 0° the robot starts making strange movements to achieve the desired coordinates which can result in reaching axis limits or collision. Also, the closer to -90° the more the effect of shaft deflection affects the actual position of tape laying. An optimal bias angle of -80° was found to lead to the most efficient robot movements.

This project has received funding from the European Union's Horizon 2020 research and innovation programme under grant agreement No 952966.

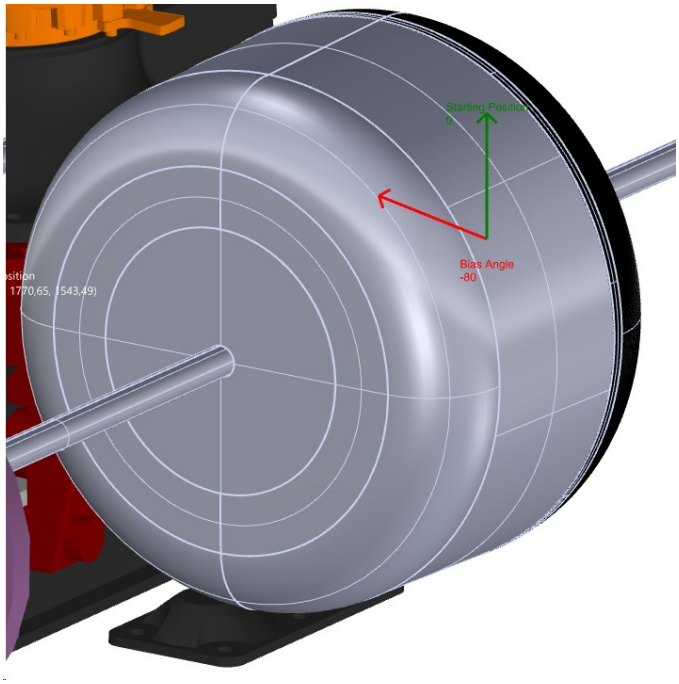

Figure 34 – Bias angle of the robot. The red axis is bias -90° and the green axis is the 0° bias angle

This project has received funding from the European Union's Horizon 2020 research and innovation programme under grant agreement No 952966.

7. PART CURING

After the deposition of all the layers, the mandrel is taken out of the robot supports and disassembled from the shafts and rims subset. The curing process follows the standard procedure of vacuum bag and oven cure commonly employed in composite laminates made from prepregs. The detailed steps for this process can be found in Figure 35.

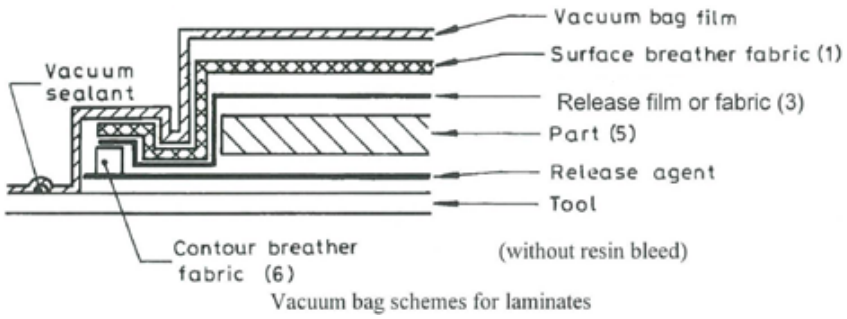

Figure 35 – Vacuum bag scheme for laminates

First, triangular strips of release fabric and surface breather fabric are cut to the curvature format of the composite. These strips are then stacked on top of the composite, completely covering it, as depicted in and Figure 37. The release fabric is stacked first, following the same order described in Figure 35.

Figure 36 – Application of release fabric

This project has received funding from the European Union's Horizon 2020 research and innovation programme under grant agreement No 952966.

Figure 37 – Application of surface breather fabric

A sheet of bagging film was cut to the length of the perimeter of the composite, and applied on the mandrel with a leeway flap for the vacuum bag, as depicted on Figure 38. The remaining length was adjusted along the curvature of the composite with loops of vacuum sealant tape.

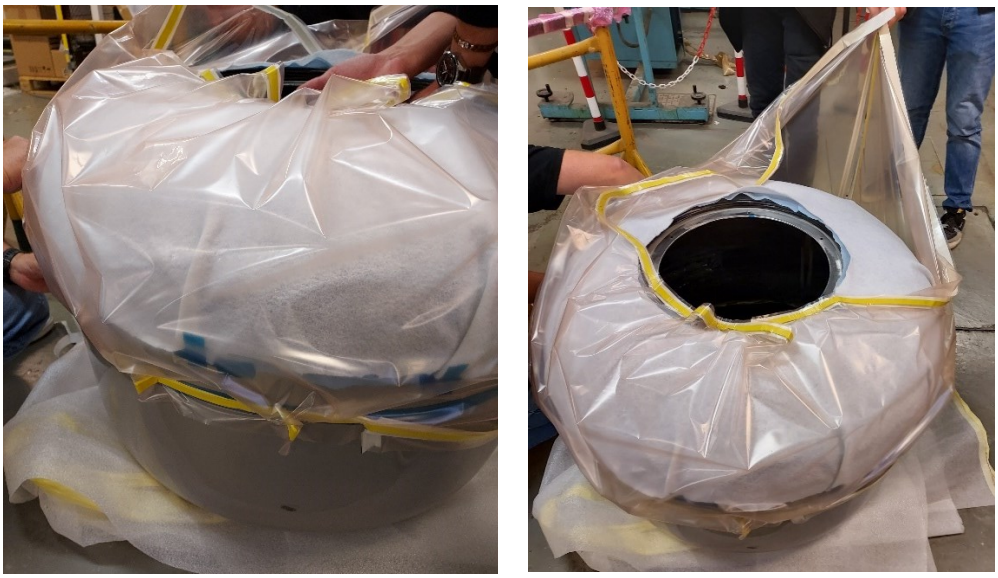

Figure 38 – Applying the vacuum bag

Before transporting the mould to the oven, vacuum was applied using the valve to check for any leaks and then the mould is placed inside the oven with the vacuum hose passing through an opening on the side, as illustrated on Figure 39.

This project has received funding from the European Union's Horizon 2020 research and innovation programme under grant agreement No 952966.

Figure 39 – Applying vacuum and inserting the mould into the oven

The curing cycle program consists of a temperature of 130℃ maintained for a duration of 2h, with a heating and cooling rate of 2℃/min. The resulting program is illustrated in the graph provided in Figure 40.

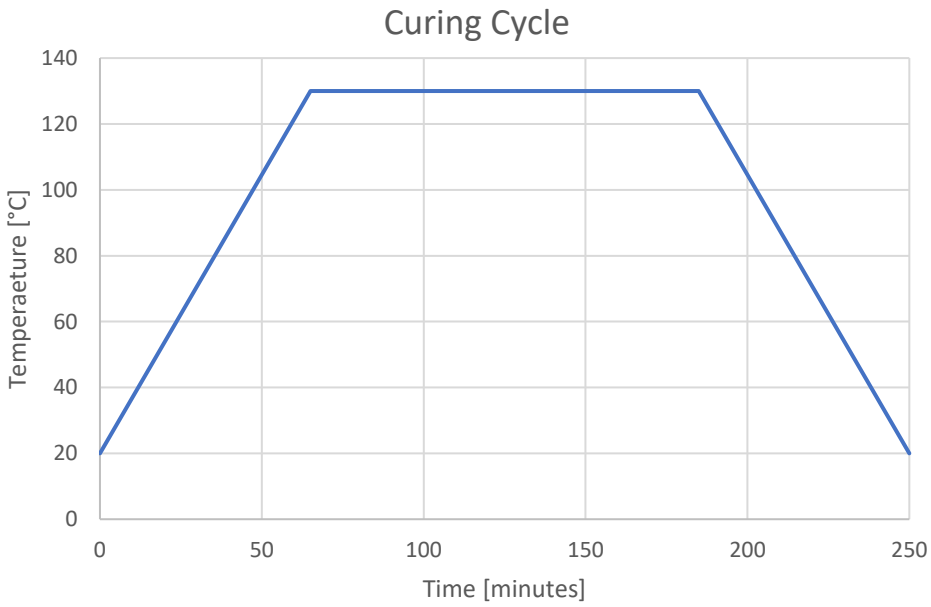

Figure 40 – Curing cycle

After curing, the mould is taken out of the oven and all the vacuum fabrics, films and tapes are removed from the composite, as depicted in Figure 41.

This project has received funding from the European Union's Horizon 2020 research and innovation programme under grant agreement No 952966.

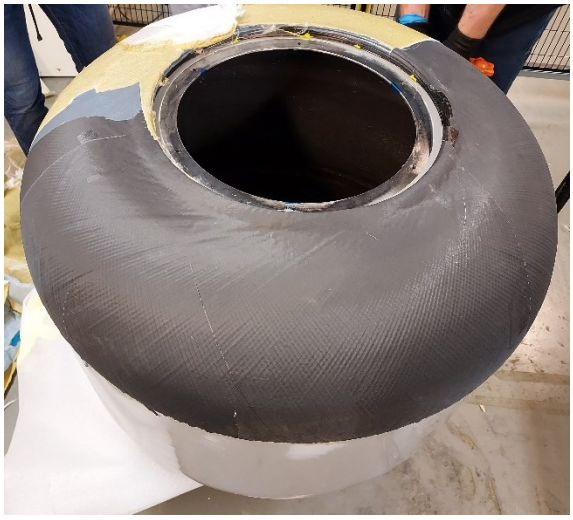
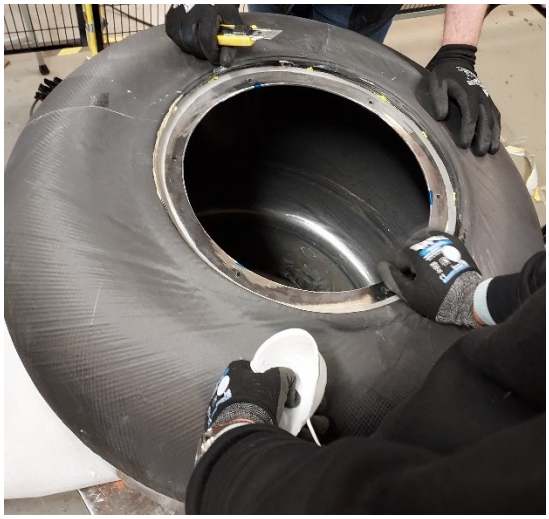

Figure 41 – Mold out of the oven and removing vacuum tools

The process for demoulding involved applying compressed air and wedges to the top part of the composite in the aperture area. Loosening the bottom part from the remaining Flashbreaker tapes and using spatula also helped during the demoulding.

The final weight of the composite is 5.6kg for the smaller lid and 8.9 kg for the larger lid. The two components, top and bottom lids are then cut so that the internal length is equal to the length of the turbine.

This project has received funding from the European Union's Horizon 2020 research and innovation programme under grant agreement No 952966.

8. FINISHING

Some cutting, trimming and sanding operations had to be done in order to cut the parts to the desired length, trim the edges of the cured parts, prepare the surfaces for bonding, and reduce the thickness in the ends thus allowing for a better placement of the fairings.

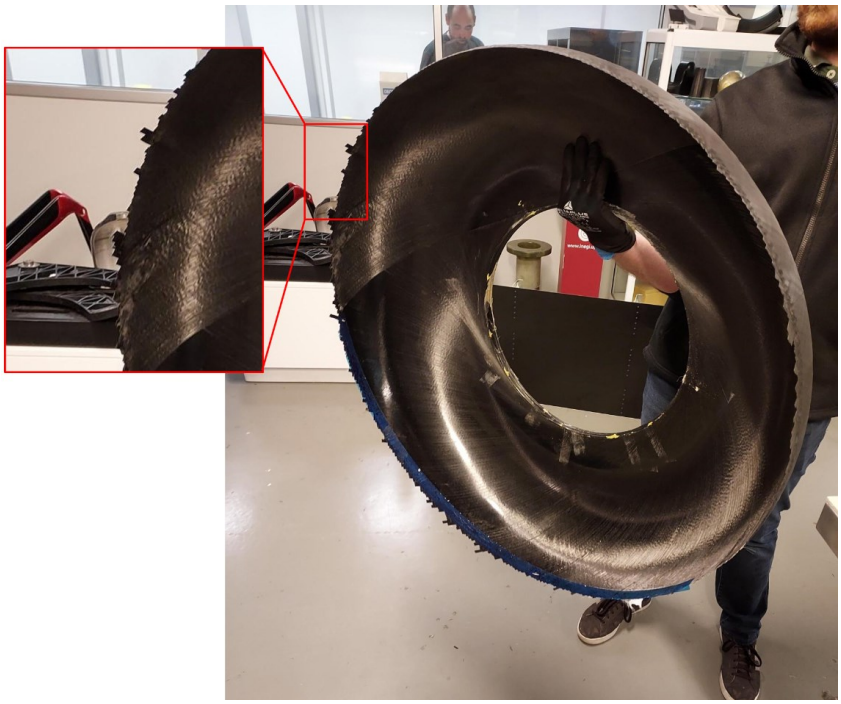

Figure 42 – Fibre edges that require trimming

These operations were manually carried out using pneumatic grinders, sanders and diamond cutting disks (Figure 43).

Figure 43 – Sanding of the ends with overthickness

This project has received funding from the European Union's Horizon 2020 research and innovation programme under grant agreement No 952966.

9. ASSEMBLY

The composite housing is placed and secured on a writable surface and the outline of the opening is marked. Using this contour, the center of the circle can be determined, enabling precise positioning of the attaching turbine bolts. The method employed utilizes the fact that the perpendicular bisector of any the cord of a circle passes through its center. By intersecting two of these lines, as depicted on Figure 44, we can identify the center of the circle accurately. The turbine bolts are inserted through ⌀17 mm holes, arranged in a circular pattern with a pitch circle diameter of ⌀504 mm. These bolts are evenly spaced at 45° angles, resulting in a total of 8 bolts.

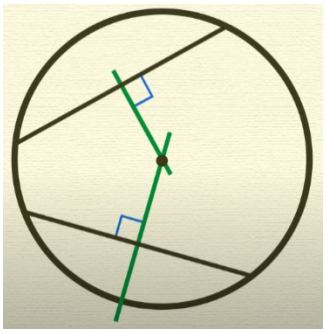

Figure 44 – Finding the centre of a circle through the perpendicular bisector of two chords

The same procedure can be applied to drill the holes on the fairings. By using aligning pins, the housing and the fairing can now be concentrically aligned during the application of glue. This ensures precise alignment between the two components.

The smaller lid is placed on the floor with the turbine on the top standing up. The first eight bolts can now be fastened. Afterward, the top lid can be placed on top of the turbine and fastened to the turbine using blind bolts, as those shown in Figure 45.

Figure 45 – Blind bolts

This project has received funding from the European Union's Horizon 2020 research and innovation programme under grant agreement No 952966.

The flanges can be positioned along the edge of the two lids and glued in to the respective lid. Another method of rotational positioning involves aligning a hole in the flange with a hole in the fairings. In this case, the flanges can be pre-glued to the housing, but careful alignment of the turbine holes is crucial between each side. Any errors in the rotational positioning are confined to the length of the ovalized hole on one of the flanges, minimizing their impact.

Figure 46 – Renderized mockup of the final assembled housing

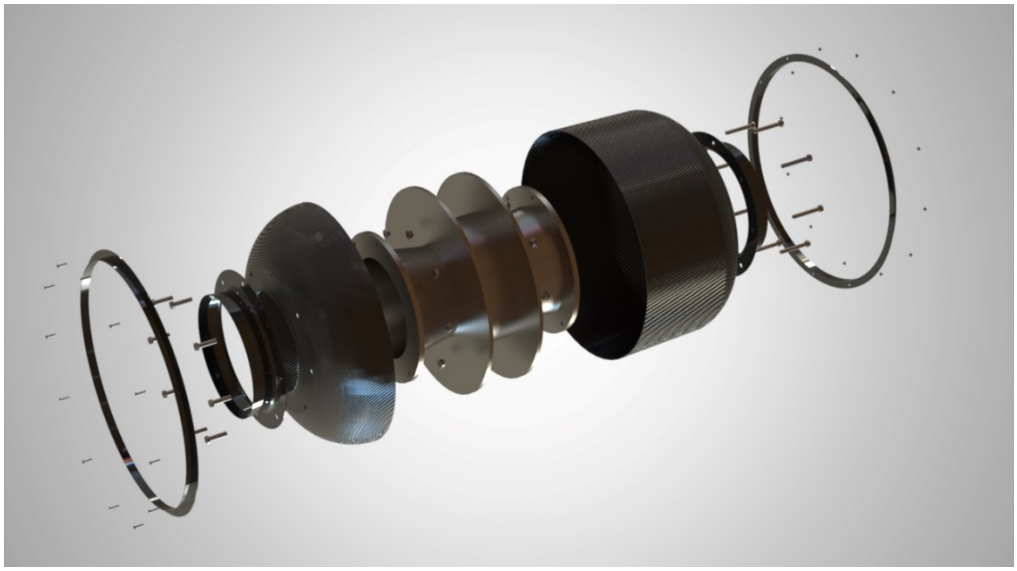

Figure 47 – Exploded view of the overall assembly

Despite the fact that at the date of submitting of this deliverable, the turbine has not yet arrived to INEGI's facilities due to constraints at the customs, the two made modules were already assembled together as well as the fairings bonded to the composite parts. The bonding

This project has received funding from the European Union's Horizon 2020 research and innovation programme under grant agreement No 952966.

operations (between the CFRP parts and the fairings and flanges) were made using the ARALDITE® 2015-1 [2], the same used in tasks 2.3 and task 6.1. It is a structural paste adhesive, extremely resistant to weathering and dynamic loading and is ideal to bond dissimilar substrates such as metal-CFRP. During bonding, masking tape was used delimiting the bonding regions, thus protecting the surfaces from unwanted adhesive.

Figure 48 – Bonding operation

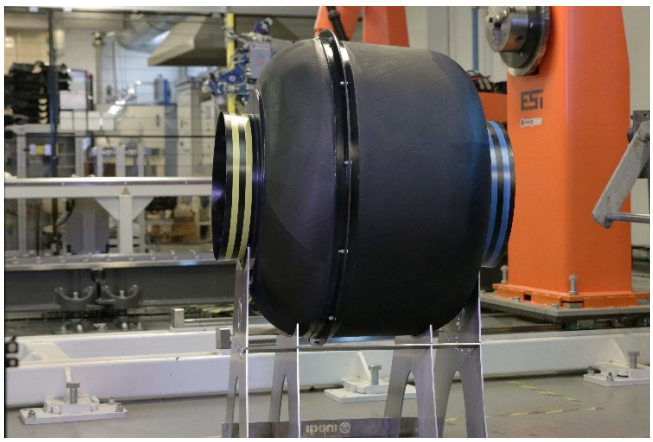

This project has received funding from the European Union's Horizon 2020 research and innovation programme under grant agreement No 952966.

Figure 49 – Assembled housing

This project has received funding from the European Union's Horizon 2020 research and innovation programme under grant agreement No 952966.

10. TESTING

10.1. Introduction

It is widely known that vibrations are the root cause of a large number of failures in structures made out of fibre reinforced polymers (FRP) such as per example aircraft, ships, wind turbines, and other engineering structures. Therefore, there is a need to control the vibratory levels of such structures to avoid undesirable resonances, cracks, and increase the life cycle of the materials.

The main objective of this research work is to investigate the vibratory behaviour of the Tidal Housing Demonstrator manufactured via Filament Winding in the context of the FIBREGY project. To achieve this goal, natural frequencies, damping, and mode shapes of the Tidal Housing Demonstrator are determined experimentally using modal analysis. This research expands the knowledge about the vibratory characteristics (natural frequencies, damping, and mode shapes) of a new generation of lightweight Tidal Housing Demonstrators made out of fibre-reinforced polymers.

Moreover, the damage attributed to the impacts is a main concern for the structural integrity of composite laminates. The other major objective of this research was to investigate the development of an impact monitoring system to monitor the external part of the prototype of the Tidal Plant based on a network of accelerometers. The results of this work revealed the capabilities of the impact monitoring system to measure impacts in real-time, which has relevant applications in structural health monitoring systems, vehicle safety, and touch screens, among others. This study provides insight into the vibratory properties of this new generation of lighter Tidal Housing Demonstrators made out of fibre-reinforced polymers. The findings of this work are of great interest to the composite industry as FRP-based laminates could be potentially used to enhance the vibratory properties of Offshore Wind Turbines and Tidal platforms.

Chapter 10.3 presents, discusses and analyses the results of the vibration assessment of the Tidal Housing demonstrator; while Chapter 10.4 addresses the validation and verification of the impact monitoring system for the Tidal Housing demonstrator. The most relevant conclusions obtained during the experimental trials will be provided together with the Chapter 11.

This project has received funding from the European Union's Horizon 2020 research and innovation programme under grant agreement No 952966.

10.2. Structure for assessment

The tests were carried out at the main body of one of the demonstrators built, as illustrated in Figure 50. It is a monolithic part CFRP, manufactured by AFP using the process already previously exposed.

Figure 50 – Photography of Tidal Housing Demonstrator tested in this study

10.3. Vibration Assessment

10.3.1. Methods

The modal parameters of the Tidal Housing Turret were provided by a modal analysis test which provides natural frequencies, damping, and vibratory mode shapes of the Tidal turbine housing. Figure 51 shows a description of the experimental set-up of the Tidal Housing. The FRP-based Tidal Turret is tested in free-free boundary conditions using a couple of elastic bundles fixed to the prototype and the whole experimental campaign were carried out on the same test rig to ensure identical free-free boundary conditions for all the tests.

The vibration tests can be divided into three steps. Firstly, a sharp impact is applied to a driving point of the Tidal Housing using a modal hammer to excite the turret. Each impact was repeated five times with the purpose to obtain a sufficient number of realizations for each test. Secondly,

This project has received funding from the European Union's Horizon 2020 research and innovation programme under grant agreement No 952966.

the vibration signals of the turret housing were recorded by B&K 4381 accelerometers in the frequency range 0 - 3000 Hz (with a frequency rate of 6 kHz). From the photography, it can be seen that the accelerometers were ubicated in the positions marked with a white band as can be seen in Figure 51.

Figure 51 – Description of the vibration test used to obtain the modal parameters of the Tidal Housing. The white bands show the position of the accelerometers during the test.

Natural Frequencies

The natural frequencies of the Tidal Housing are extracted from the recorded time domain response using the Fast Fourier Transform (FFT) [3]. The distinct peaks in the FFT spectrum are associated with each of the natural frequencies of the Tidal Housing. Each impact was repeated five times with the fundamental purpose to obtain multiple realizations for each test. The standard deviation of the natural frequencies from the five measurements is practically zero which indicates that the values of the natural frequencies are rather stable.

Damping

The damping is a parameter associated with the capabilities of a material for reduction of the vibratory levels over some time and therefore, a good indicator of the capability of a material to dissipate vibrational energy. The damping of the principal natural frequencies of the composite turret housing was calculated using the half-power method [5]. Equation (1) can also be efficiently used for the evaluation of the capability of FRP-based turret for dissipation of energy.

This project has received funding from the European Union's Horizon 2020 research and innovation programme under grant agreement No 952966.

$$\zeta = \frac{w_3 - w_1}{2w_2} \qquad (1)$$

where w_1, w_2, and w_3 are the frequencies associated with the first, second, and third points of the frequency spectrum shown in Figure 52. From the figure, it is appreciated that w_2 can be defined as the frequency of the resonant peak while w_1 and w_3 stands for the points of the peak located 3 dB below the maximum amplitude.

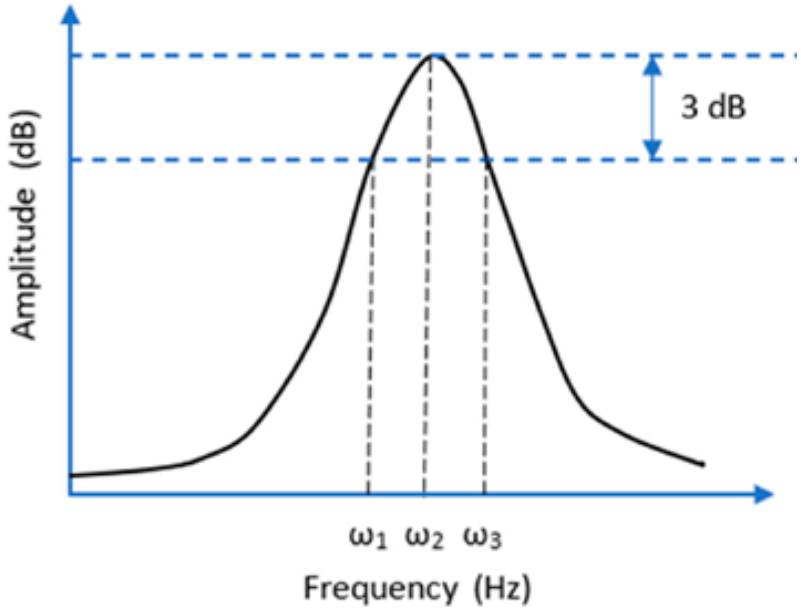

Figure 52 – Half power damping method used for calculation of damping

Vibrational Mode Shapes

A vibrational mode shape is a deflection pattern related to a particular natural frequency and represents the relative displacement of all parts of a structure for that particular mode [6]. Therefore, mode shapes can be defined as a manifestation of eigenvectors which describe the relative displacements of elements part of a mechanical system.

The vibration mode shapes of the first five modes of the Tidal Turret housing are determined through a modal analysis tool using the vibration analysis software Siemens LMS Test Lab. In this research, the first five vibration mode shapes of the Tidal Turret are investigated with the Modal Analysis Module of Siemens LMS Test Lab.

This project has received funding from the European Union's Horizon 2020 research and innovation programme under grant agreement No 952966.

10.3.2. Results and Discussion

The results obtained in the vibration tests of the FRP-based Tidal housing are presented and discussed in the context of Chapter 10.3. Below, three subsections show information about the natural frequencies, damping, and vibration mode shapes of the Tidal Turret.

Natural Frequencies

This section looks at the natural frequencies of the FRP-based tidal housing used for the construction of the Tidal Plant, with the fundamental purpose to provide a baseline of the modal parameters when the FRP turret is in a healthy state. To address this investigation, the natural frequencies at the X, Y, and Z axis are measured to find out the effect of replacing steel with composite.

Table 2 presents a summary of the first five natural frequencies of the Tidal Turret Housing constructed for the demonstrator of WP6. The table reveals that the natural frequencies for the first five modes of the Tidal Housing turret are 403.1; 500.3; 526.9, 898.0; and 1027.3 Hz. It should be highlighted that the table also provides an average value of the natural frequencies for the experimental trials carried out in the measurement campaign. The minuscule changes in the natural frequencies with standard deviations below 5% are within the range of the experimental and measurement error.

Table 2 – Values of the natural frequencies obtained via Modal Analysis.

Mode	Test 1 (Hz)	Test 2 (Hz)	Test 3 (Hz)	Test 4 (Hz)	Test 5 (Hz)	Test 6 (Hz)	Test 7 (Hz)	Test 8 (Hz)	Average (Hz)	SD (Hz)
1	403.1	403.1	403.1	403.1	403.1	403.1	403.1	403.1	403.1	0.00
2	496.8	500.0	503.1	503.1	503.1	496.8	500.0	500.0	500.3	2.44
3	525.0	531.2	521.8	525.0	525.0	528.1	528.1	531.2	526.9	3.10
4	896.8	900.0	900.0	896.8	896.8	900.0	896.8	896.8	898.0	1.51
5	1028.1	1028.1	1031.2	1031.2	1018.7	1025.0	1025.0	1031.2	1027.3	4.06

The findings of this research are in line with other works previously reported in the literature. For example, K. Alnefaie [7] reported that the variations of the natural frequencies for tests carried out for various FRP plates with different delamination patterns are minuscules. In parallel, other authors as [8-9] investigated the effect of the apparition of internal defects on the natural

This project has received funding from the European Union's Horizon 2020 research and innovation programme under grant agreement No 952966.

frequencies, however the shift of the natural frequencies for the natural frequencies with and without delamination patterns do not surpass 5%.

For this particular case, the shift of the natural frequencies is attributed to the stiffness variation due to the damage caused by the delamination failures. Other research projects [10] investigated the change of the natural frequencies due to the substitution of FRP for steel, where it can be appreciated a shift of the natural frequencies and a drastic weight reduction. In general, it can be concluded that the substitution of steel by FRP produce a shift in the natural frequencies which leads to a global reduction of the natural frequencies of the structures.

Damping

The damping represents the amount of energy that can be dissipated by a material after an external excitation. The higher the damping, the greater the capabilities of a material to dissipate vibrational energy, which is an application of interest for components where vibrations are a source of problems. This is beneficial as higher damping materials can be used to reduce the vibration amplitudes in structures and alleviate the effect of resonances.

Table 3 presents the values of the damping for the first five modes of the Tidal Turret Housing, which were calculated using the Half Power Damping Method. The table reveals that the average values of the damping are 0.51, 0.61, 0.37, 0.42, and 1.01 for the five modes of the natural frequencies. The standard deviations for the damping values vary in the range from 0.03 - 0.59.

Table 3 – Values of the Damping obtained via Modal Analysis

Mode	Test 1 (Hz)	Test 2 (Hz)	Test 3 (Hz)	Test 4 (Hz)	Test 5 (Hz)	Test 6 (Hz)	Test 7 (Hz)	Test 8 (Hz)	Average (Hz)	SD (Hz)
1	0.50	0.45	0.54	0.51	0.51	0.50	0.47	0.56	0.51	0.03
2	0.44	0.41	2.18	0.44	0.39	0.32	0.34	0.39	0.61	0.59
3	0.36	0.36	0.39	0.42	0.56	0.35	0.34	0.21	0.37	0.09
4	0.45	0.38	0.40	0.36	0.50	0.39	0.33	0.52	0.42	0.06
5	1.24	0.82	1.39	1.58	1.14	0.97	0.53	0.44	1.01	0.38

In general, it is noticed that the damping values of FRP-based materials are greater than the damping of steel ones. For example, the authors of [11] demonstrated that the damping of a 1000 mm-lenght steel beam is 0.42, while the damping for an identical size FRP-based plate is 1.01, and therefore, there is an increment of 2.4 times damping. The tendency shows an identical tendency for other vibration mode shapes with increments in the range of 2-5 times more. The main reason

This project has received funding from the European Union's Horizon 2020 research and innovation programme under grant agreement No 952966.

for the increments is that the heterogeneous structure of a composite laminate increases the damping levels due to the multiple composite interfaces which act as dampers to enhance the dissipation of energy.

Mode Shapes

Another parameter analysed by the research team are the vibration mode shapes of the Tidal Turret Housing. Modes 1 and 4 of the Tidal Housing are represented in the context of Figure 53. assemblThe first and second mode of the vibration mode shapes are represented in the upper part of the figure, while the third, and forth mode are shown in the bottom part.

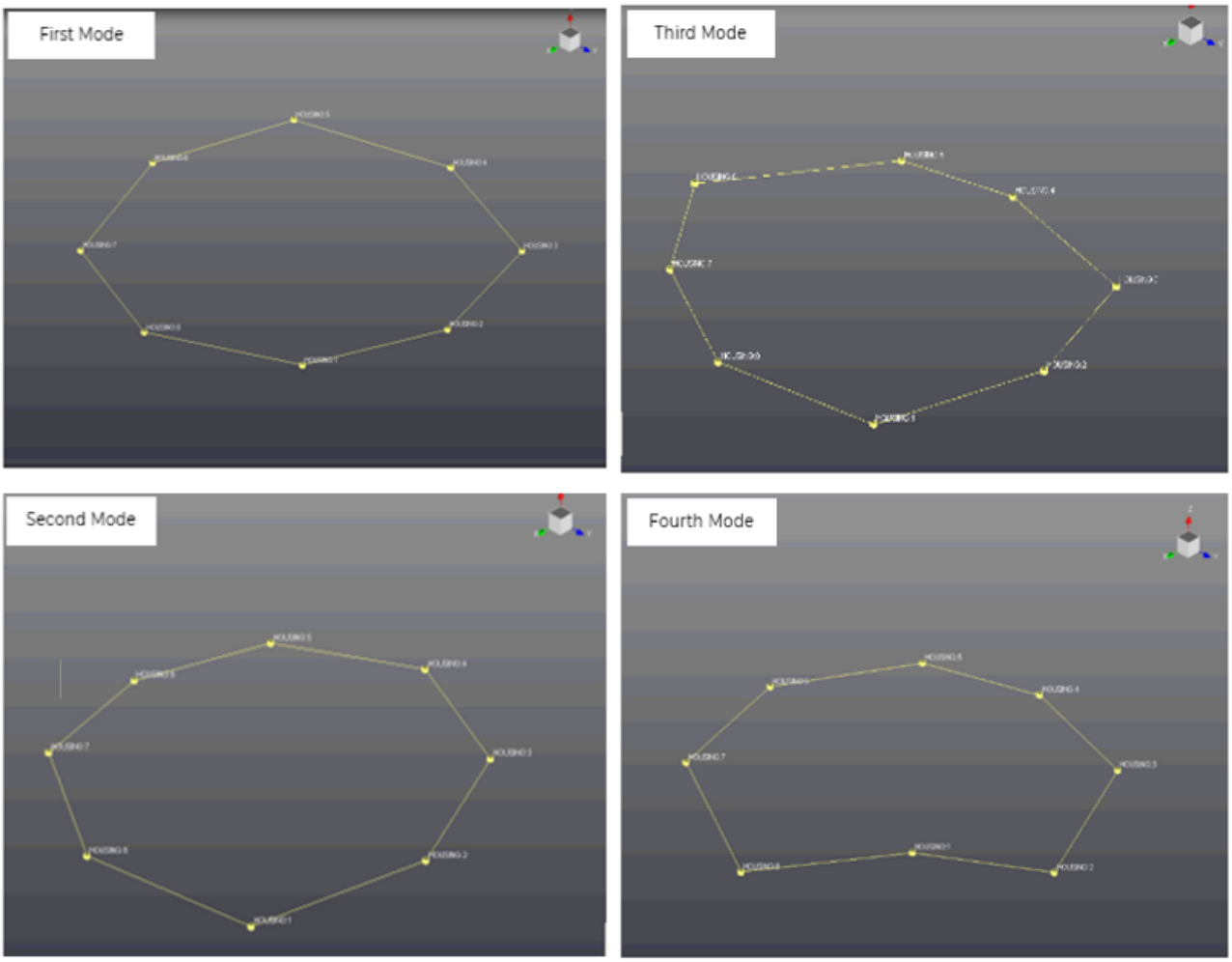

Figure 53 – Description of the first fourth mode shapes of the Tidal Turret Turbine.

This project has received funding from the European Union's Horizon 2020 research and innovation programme under grant agreement No 952966.

10.4. Impact Assessment

10.4.1. Methods

An impact monitoring system plays a pivotal role in airbag monitoring systems, rapid medical assistance of falls, along with structural health monitoring systems of engineering structures. Within the automotive industry, an impact sensor serves to detect collisions with the purpose to release an airbag for the protection of the passengers in a car crash. If we look at healthcare applications, an impact sensor can be used for the detection of collisions in elderlies with the purpose to carry out rapid medical assistance in an emergency case. With regards to SHM applications, it is noticed that the detection and quantification of impacts is of relevance importance for inspection and monitoring of the health state of composite structures.

The aim of the impact tests carried out in this work is to investigate the efficiency of an impact monitoring system for the detection and quantification of energy impacts using the amplitude responses of an array of acceleration sensors. To address the tests, the Tidal Housing are subjected to controlled energy impacts using an impact tester, while the sensor electric responses are measured in time and frequency domain with a data acquisition system.

Figure 54 displays a schematic representation of the impact tests carried out during the experimental trials. The methodology used for the detection of impacts can be divided into the following two steps: Firstly, a 200 g metallic ball impacts at the turret housing with different heights which vary from 5 to 60 cm with intervals of 5 cm. Secondly, the time responses of the accelerometer are recorded with the purpose to investigate the matematical relationship between sensor amplitude electric outputs and the energy of the impacts. In short, it can be said that the main idea behind the experimental testing campaign is to investigate the relationship between the impact energy and the accelerometer electrical responses.

This project has received funding from the European Union's Horizon 2020 research and innovation programme under grant agreement No 952966.

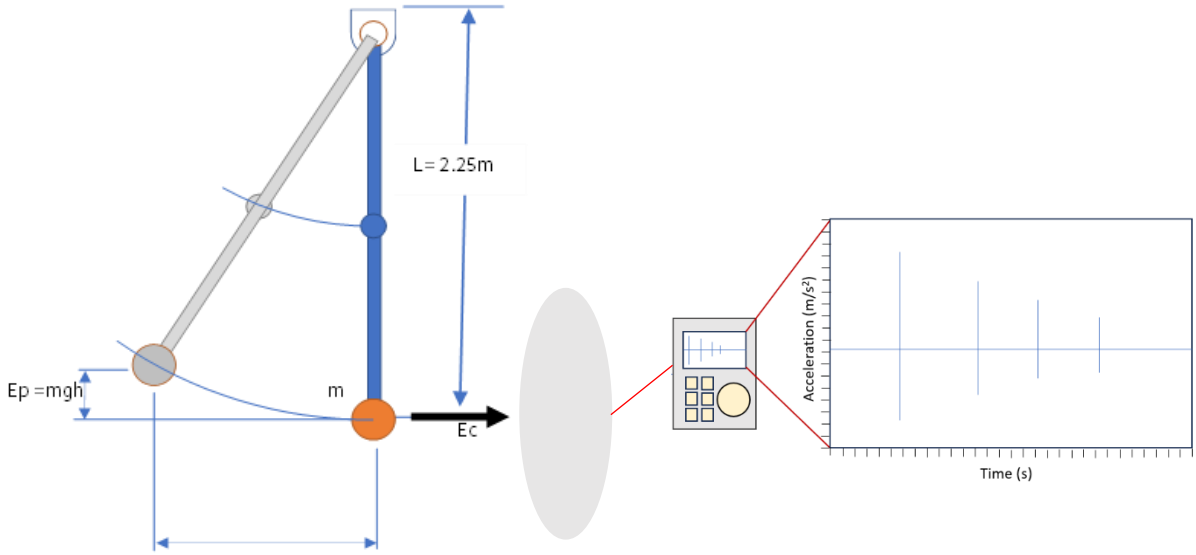

Figure 54 – Description of impact tests used to evaluate the capabilities of the monitoring system for detection of impacts at different energy levels.

A digital photography of the experimental setup can be appreciated in Figure 55. During the realization of this work, it has been used a simple set-up which consist of a metal ball, a pendule, and an accelerometer connected to a data acquisition system to record the excitations. From the figure, it can be appreciated how the height of the impacts can be easily incremented using the height indication near the turret. For this reason, it can be said that the impact tests are a simple a rapid way to evaluate the sensitivity of the monitoring system for detection and quantification of impacts at different energy levels.

This project has received funding from the European Union's Horizon 2020 research and innovation programme under grant agreement No 952966.

Figure 55 – Photography of tests used to evaluate the capabilities of a SHM system for the detection of impacts at low velocity impact energy levels

10.4.2. Results and Discussion

The experimental procedure described in Chapter 10.4.1 is used to supply energy impacts at different energy levels of the Tidal Housing. The sections below investigate the effect of the impact height on the acceleration responses.

Effect of the impact height on acceleration response

The main idea behind this experiment is to find out how the energy of the impacts influences the electric responses of the sensor. Figure 56 reveals the acceleration signals when a metallic ball with a weight of 200 g impacts at a specific location of the turret housing. The ball impacts the component from multiple heights which goes from 5 cm to 60 cm with height intervals of 5 cm.

This project has received funding from the European Union's Horizon 2020 research and innovation programme under grant agreement No 952966.

In general, it is observed that when the ball is dropped from a higher altitude, the amplitude of the acceleration increases up to 12 g. For this particular case, it is noticed that the peak-to-peak amplitude increases gradually from 0.690 g to 12.5 g as the drop height increases from 5 to 60 cm.

Apart from that, it can be appreciated a strong linear relationship amplitude-impact height with a Pearson coefficient of 0.98. Thus, a high linear relationship between the impact energy and the corresponding acceleration responses is appreciated for the range of impact heights tested. This experimental trend is in good agreement with previous research works. For example, the research publication from [12] observed that the voltage and current sensor responses are directly proportional to the energy of the impacts for the range of energies from 1 to 30 J. Similar results are shown in the research works [13], where a sensor developed for the purposes of impact monitoring was tested under high acceleration energy impacts.

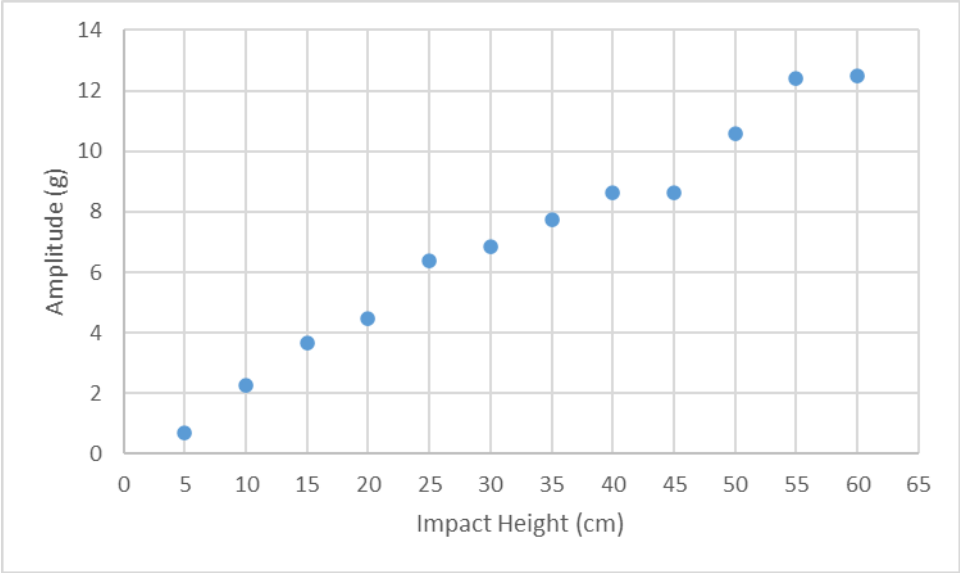

Figure 56 – Acceleration Amplitude as a function of the Impact Height for the different ball impacts.

The upper section of Figure 57 reveals the time response recorded by an accelerometer due to an external impact with an impact hammer. From the data reported in the figure, it can be clearly seen that the amplitude of the free decay response decreased from 3.5 g to 0.2 g, which gives a good indication about the high damping of the material. The bottom section of Figure 57 represents a typical FFT spectrum with first modes of the natural frequencies where it can be seen frequencies at 46.76 Hz; 71.80 Hz; 91.29 Hz; 190.09 Hz and 295.85 Hz among others. As compared to the other case scenario, It should be noted that the FRP turret specimen is clamped to the floor, and therefore, this implies a variation of the natural frequencies.

This project has received funding from the European Union's Horizon 2020 research and innovation programme under grant agreement No 952966.

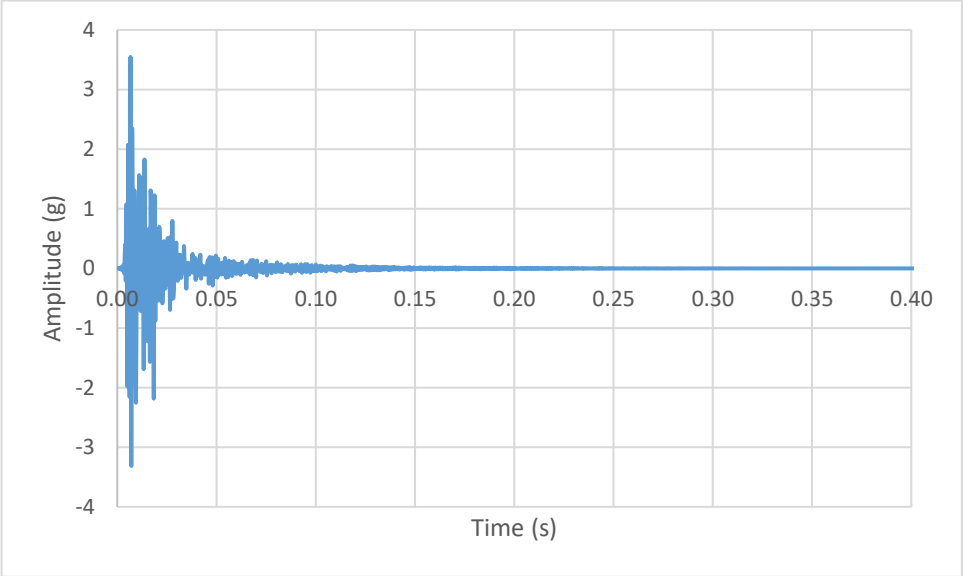

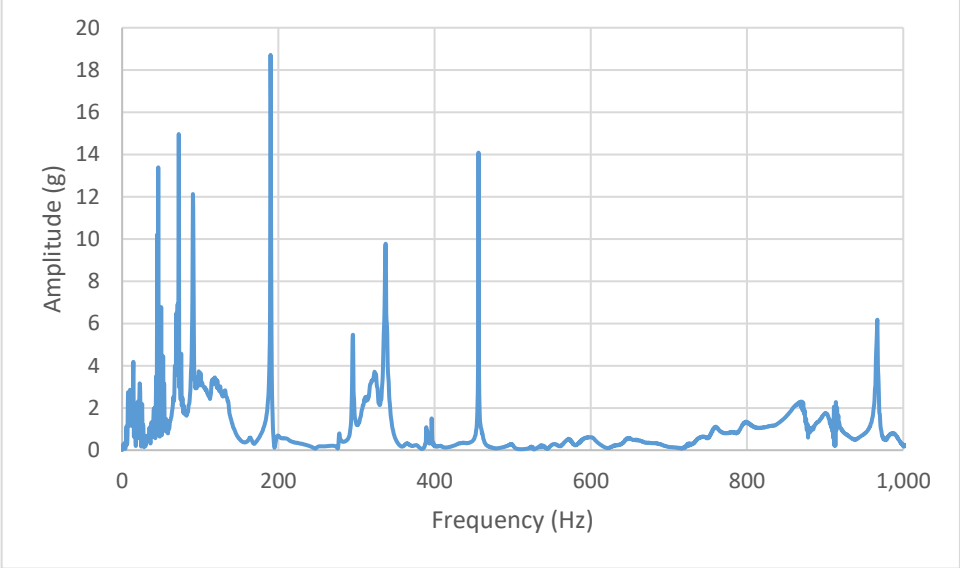

Figure 57 – Acceleration responses due to an impact and Fast Fourier Spectrum of the Tidal Turret.

This project has received funding from the European Union's Horizon 2020 research and innovation programme under grant agreement No 952966.

11. CONCLUSIONS

The construction of the turbine housing demonstrator within the FIBREGY project marks a significant milestone in the pursuit of innovative renewable energy solutions made of FRP. Through meticulous planning, iterative design processes, and strategic implementation of cutting-edge manufacturing techniques, this deliverable has successfully demonstrated the feasibility and advantages of composite construction for the turbine housing, particularly using Automated Fibre Placement (AFP), a pivotal choice to reduce manual labour, thereby mitigating the risk of human errors and ensuring consistent quality in the final product.

The challenges of re-designing the housing and its mandrel – using DfM principles in order to ensure the manufacturability – were well described and will be an important input for future manufacturers, being a particularly useful contribution for the deliverable 5.4 ("Guidance notes for the production of large FPR OWTP") to be submitted next month. It is also significant to mention that this design, which is for the demonstrator size, can also be scaled up to a real-sale concept (although changes to the manufacturing process are likely to be needed).

The preparation steps of the manufacturing, which included the coding and parameterization of the program for the robot, were also explained, together with the difficulties faced and the necessary optimizations. Being a novel process and still in a maturing phase, these observations will be important for further revisions of the software and also the robot head equipment.

Concerning the testing assessments, this research study has considered the vibratory behaviour of FRP-based components, which are used for the design and construction of Tidal Power Plants. To evaluate the vibratory behaviour of the Tidal Turret, the modal parameters (natural frequencies, damping, and mode shapes) of the turret are investigated. The project results demonstrated that the utilization of FRP instead of steel implies a drastic weight reduction and therefore, a shift of the natural frequencies.

Furthermore, this work presents solid progress toward the practical implementations of accelerometers for the detection of low-velocity impacts in FRP-based turret components. The findings of this study demonstrate that the accelerometers can be potentially used for the detection of impacts exerted by an impact tester, which can have relevant applications for the detection of impacts in composite structures such as aircraft, bridges, and other composite structures. An interesting linear relationship between the impact height and the peak-to-peak amplitude of the acceleration responses has been found.

This project has received funding from the European Union's Horizon 2020 research and innovation programme under grant agreement No 952966.

12. REFERENCES

[1] Tidetec, "Superior turbine efficiency enabled by the turning mechanism and its integration with the optimized turbine and caisson." https://tidetec.com/technology/.

[2] Huntsman International LLC., "ARALDITE® 2015-1." https://www.huntsman.com/products/araldite2000/araldite-2015-1.

[3] N. Rahman, An efficient method for frequency calculation of an audio signal, Presidency, 2 (2013) 41-45.

[4] L.B. Magalas and T. Malinowski, Measurement Techniques of the Logarithmic Decrement, J Solid State Phenom., 89 (2013) 247-260.

[5] S. Carmichael, Estimating Damping Values Using the Half Power Method, Integrated Systems Research, 2015.

[6] G. Moraga, M. Egusquiza , D. Valentín , C. Valero, and A. Presas, Analysis of the Mode Shapes of Kaplan Runners, Appl. Scie., 12 (2022) 6708.

[7] K. Alnefaie, Finite element modelling of composite plates with internal delamination, Compos. Struct., 90 (2009) 21-27.

[8] T. Mukhopadhyay, S. Naskar, P.K. Karsh, S. Dey, Z. You, Effect of delamination on the stochastic natural frequencies of composite laminates, Composites Part B: Engineering, 154 (2018) 242-256.

[9] G. Minak, R. Palazzetti, I. Trendafilova, and A. Zucchelli, Localization of a delamination and estimation of its length in a composite laminate beam by the VSHM and pattern recognition methods, Mech Mater., 46 (2010) 387-394.

[10] Min-Jae Kim, Jung-Hoon Lee, Seok-Ho Kim, Choon-Man Lee, and Dong-Hyeon Kim, Comparative Analysis of CFRP and Steel Vibration Characteristics of Machine Tools Components, Applied Sciences, 13 (2023) 1083.

[11] V. Dacol, E. Caetano, and J.R. Correia, Comparative Study of Damping on Pultruded GFRP and Steel Beams, Polymers, 13 (2021) 2201.

[12] C. Garcia, I. Trendafilova, J. Sanchez del Rio, Detection and measurement of impacts in composite structures using a self-powered triboelectric sensor, Nano Energy, 56 (2019) 443-453.

[13] K. Dai, X. Wang, F. Yi, C. Jiang, R. Li, Z. You, Triboelectric nanogenerators as self-powered acceleration sensor under high-g impact, 45 (2018) 84-93.